Environmental Science: Atmospheres

ROYAL SOCIETY OF CHEMISTRY

CRITICAL REVIEW

View Article Online
View Journal



Cite this: DOI: 10.1039/d6ea00017g

# Peroxyacetyl nitrate (PAN) in the atmosphere: a comprehensive review of chemistry, measurements, and chemical-transport implications

Callum E. Flowerday and Jaron C. Hansen*

Peroxyacetyl nitrate (PAN) is a secondary pollutant formed through the photochemical oxidation of volatile organic compounds (VOCs) in the presence of nitrogen dioxide ($NO_2$). Since its identification in 1956, PAN has been recognized as a major reservoir for nitrogen ($NO_x$) and a component of photochemical smog and $NO_y$. Its thermal instability makes PAN lifetimes highly temperature dependent, with lifetimes ranging from minutes in the warm boundary layer to months in the upper troposphere. This behavior allows PAN to transport $NO_x$ efficiently over regional and intercontinental scales, influencing downwind ozone ($O_3$) formation, oxidant cycling, and nitrogen deposition far from emission sources. PAN is lost primarily through thermal decomposition, with slower removal *via* photolysis, heterogeneous uptake, and minor reactions with OH and Cl. It correlates strongly with $O_3$, responds nonlinearly to precursor changes, and its formation is often VOC-limited in urban regions. While PAN decomposition can enhance downwind $O_3$ formation, PAN is also toxic in its own right, functioning as a potent lachrymator and phytotoxin that directly impacts human health and vegetation. Biomass burning, haze chemistry, and free-tropospheric transport further modulate PAN abundance and seasonality. This review synthesizes the current understanding of PAN chemistry, sources, and loss pathways; evaluates historical and modern measurement techniques; and examines PAN's role in photochemical smog, air quality, vegetation injury, and regional background $O_3$. Key uncertainties, including heterogeneous processing, indoor chemistry, and climate-driven shifts in PAN formation, are highlighted as priorities for future research. A general analysis of the literature and future research directions is discussed.

Received 31st January 2026
Accepted 1st May 2026

DOI: 10.1039/d6ea00017g

rsc.li/esatmospheres



### Environmental significance

Peroxyacetyl nitrate (PAN) plays a central role in transporting reactive nitrogen and regulating ozone formation across urban, regional, and remote environments. Despite decades of study, inconsistent measurement approaches and interpretations of PAN chemistry continue to introduce uncertainty into assessments of nitrogen oxide lifetimes, photochemical ozone production, and model performance. By critically evaluating observational methods, chemical processes, and environmental implications, this review clarifies how improved treatment of PAN can strengthen air-quality analysis and atmospheric chemistry models under present and future climate conditions.

## 1 Introduction

### 1.1 History

Peroxyacetyl nitrate (PAN, $C_2H_3O_5N$), also known as peroxyacetic nitric anhydride or acetic nitric peroxyanhydride, has been considered an important atmospheric constituent since its first detection in Los Angeles smog in 1956 using long-path infrared spectroscopy.[1–4] Early smog investigations in 1940–1950s southern California, motivated by severe eye irritation, rubber cracking, reduced visibility, and widespread crop damage, led researchers such as Haagen-Smit, Middleton, Darley, Stephens, and others to search for the unknown oxidants responsible for "photochemical smog".[5,6] Long-path IR measurements in the mid-1950s revealed unusual absorption features belonging to a mysterious "Compound X," and subsequent work ultimately confirmed its identity as PAN.[4–6]

Later, advances in analytical techniques, such as gas chromatography with electron capture detection (GC-ECD), enabled routine PAN quantification at ambient levels,[7] while early mass spectrometry provided structural confirmation. Synthetic methods progressed from photolysis of ethyl nitrite and dark nitrogen pentoxide ($N_2O_5$) + acetaldehyde reactions to strong-acid nitration of peracids with extraction into low-volatility solvents such as tridecane.[8] These developments produced

*Department of Chemistry and Biochemistry, Brigham Young University, Provo, UT, USA. E-mail: jhansen@chem.byu.edu*

stable, high-purity PAN standards and made PAN measurements accessible to atmospheric chemists around the world.

As measurement technology improved, it became clear that PAN was more than a local smog irritant. PAN was detected globally[8] and recognized as a major long-range reservoir for $NO_x$, a potent phytotoxin, and a key player in the chemistry governing photochemical smog and downwind ozone ($O_3$) formation. The discovery of PAN in remote marine environments further established its global importance.[9] Today, PAN is understood as both a diagnostic marker of photochemical processing and a central component of reactive nitrogen cycling.

The past two decades have seen major advances in high-time-resolution measurement techniques, satellite retrieval capability, multiphase chemistry understanding, and global chemical transport modeling. This review therefore places particular emphasis on integrating these modern developments with historical knowledge to provide an updated synthesis of PAN's role in the contemporary atmosphere.

### 1.2 Background

PAN is formed almost entirely *in situ* through the photochemical oxidation of non-methane hydrocarbons (NMHCs) in the presence of nitrogen dioxide ($NO_2$), and is the first and most abundant member of the peroxyacyl nitrate (PAN) family, which includes species such as peroxypropionyl nitrate (PPN) and peroxymethacryloyl nitrate (MPAN), and other homologous peroxyacyl nitrates.[10,11] Photooxidation of NMHCs produces peroxyacetyl radicals ($CH_3C(O)O_2$), which then combine with $NO_2$ to form PAN.[12–16] PAN is an important constituent of reactive nitrogen species ($NO_y = NO_x + HNO_3 + PAN + PANs$)[17] and can contribute significantly to the $NO_y$ budget in many regions.[10,18–23]

PAN's atmospheric behavior is controlled primarily by temperature-dependent thermal decomposition in the lower troposphere[24–26] and by photolysis at higher altitudes.[27] It reacts slowly with hydroxyl radicals (OH) and chlorine radicals (Cl)[28–30] and is stable to heterogeneous loss.[31,32] Because PAN's lifetime increases dramatically at low temperatures, it can serve as a major $NO_x$ reservoir in cold environments and can account for 50–90% of $NO_y$ under such conditions.[33,34] Aircraft observations indicate that PAN constitutes roughly 30% of $NO_y$ near 10 km altitude.[35]

Strong positive correlations between PAN and $O_3$ have allowed PAN to be used to infer background $O_3$,[36–41] and PAN is often considered a better indicator of photochemical smog than $O_3$ itself.[34,42,43] Because PAN is thermally stabilized at night, it often persists longer than $O_3$ under identical conditions.[44]

### 1.3 Health and vegetation effects

PAN has long been recognized as a potent eye irritant and strong phytotoxin.[1,34,45] It is a lachrymator, causing tearing and discomfort at very low concentrations, and early smog-era plant damage, including the characteristic "bronzing" of leaves, was directly attributed to PAN.[4,46] Controlled studies show that PAN causes cell injury in plant tissues,[47–49] with stomatal uptake rates of 20–55 pmol $m^{-2}$ $s^{-1}$ at 250 pptv.[50] Approximately 3% of global $NO_x$ emissions may be removed *via* foliar PAN uptake, and PAN deposition can account for up to 20% of total nitrogen deposition in some regions, with ~80% of PAN-derived nitrogen retained within leaves.[50]

Toxicological studies in animals show that PAN causes severe lung damage and respiratory tract irritation at sufficiently high concentrations,[51] with human eye irritation occurring at ~0.64 mg $m^{-3}$ after 2 hours. PAN is considered a weak mutagen,[52,53] but available data remain insufficient to assess carcinogenicity or chronic health risks in humans.

Beyond acute vegetation injury, PAN also plays a broader role in ecosystem nitrogen cycling. Early smog studies identified PAN as a potent phytotoxic oxidant capable of causing foliar damage and reduced crop productivity at elevated concentrations.[1–4,34,45] Subsequent experimental work has demonstrated that PAN uptake can induce cellular injury and physiological stress responses in plants.[47–49] Because PAN acts as a thermally labile reservoir of reactive nitrogen, its deposition and decomposition contribute to nitrogen inputs in terrestrial ecosystems, with foliar uptake alone accounting for several percent of global $NO_x$ removal and up to ~20% of total nitrogen deposition in some regions.[54] These interactions highlight the importance of PAN not only as an atmospheric oxidant but also as a mediator linking photochemical pollution to ecosystem nutrient dynamics.

## 2 Atmospheric chemistry

This section focuses on the chemical mechanisms governing PAN formation and loss after emission of precursor species, independent of their source origin. PAN plays a central role in tropospheric oxidant chemistry because it is both a product of VOC–$NO_x$ photochemistry and a major reservoir for reactive nitrogen. PAN's atmospheric behavior is governed by temperature-dependent thermal decomposition, the rates of its formation reactions, and its comparatively slow removal through photolysis, OH reaction, and deposition. Together, these processes determine its lifetime, spatial distribution, and influence on $O_3$ and oxidant budgets.

### 2.1 Chemical reactions

**2.1.1 Formation.** PAN formation is governed by coupled $NO_x$–NMHC chemistry that characterizes photochemical smog. Peroxy radicals ($RO_2^{\bullet}$) are produced from the photooxidation of biogenic and anthropogenic VOCs, and NO is readily available in most polluted and many rural environments. The reaction of ($RO_2^{\bullet}$) with NO forms $NO_2$:

$$RO_2^{\bullet} + NO \rightarrow RO^{\bullet} + NO_2$$

In the presence of sunlight, $NO_2$ photolysis produces tropospheric $O_3$ *via* the sequence:

$$NO_2 + h\nu \rightarrow NO + O$$

$$O + O_2 + M \rightarrow O_3$$

Peroxyacetyl radicals ($CH_3C(O)OO^{\bullet}$) are formed through the photooxidation of a range of organic compounds, including isoprene and carbonyls. Major precursors include acetaldehyde, acetone, methylglyoxal, biacetyl, and other ketones with the generic structure $CH_3C(O)R$.[55] Reaction of $NO_2$ with the peroxyacetyl radical yields PAN:

$$CH_3C(O)CH_3 + 2O_2 + h\nu \rightarrow CH_3C(O)OO^{\bullet} + CH_3O_2$$

$$CH_3C(O)C(O)CH_3 + 2O_2 + h\nu \rightarrow 2CH_3C(O)OO^{\bullet}$$

$$CH_3CHO + O_2 + NO_3 \rightarrow CH_3C(O)OO^{\bullet} + HNO_3$$

$$NO_2 + CH_3C(O)OO^{\bullet} \rightarrow CH_3C(O)OONO_2$$

PAN can also be formed through the OH-initiated oxidation of acetaldehyde in the presence of $O_2$ and $NO_2$,[56,57]

$$CH_3CHO + OH \rightarrow CH_3CO^{\bullet} + H_2O$$

$$CH_3CO^{\bullet} + O_2 \rightarrow CH_3C(O)OO^{\bullet}$$

$$NO_2 + CH_3C(O)OO^{\bullet} + M \rightarrow CH_3C(O)OONO_2 + M$$

This sequence competes with the direct conversion of NO to $NO_2$ by peroxyacetyl radicals:[58]

$$NO + CH_3C(O)OO^{\bullet} \rightarrow CH_3C(O)O^{\bullet} + NO_2$$

$$NO + CH_3C(O)OO^{\bullet} \rightarrow CH_3^{\bullet} + CO_2 + NO_2$$

$$NO + CH_3C(O)OO^{\bullet} + O_2 \rightarrow CH_3O_2 + CO_2 + NO_2$$

followed by rapid secondary oxidation of $CH_3C(O)O^{\bullet}$.[56,57] Competition between PAN formation and NO oxidation therefore directly couples PAN production to the local $NO/NO_2$ ratio.

In polluted urban environments, PAN formation is approximately proportional to $[NO_2]$ and competes with peroxyacetyl radical reactions with NO.[56] Under these conditions, the steady-state PAN concentration scales with $[NO_2]/[NO]$. Because $O_3$ steady-state concentrations also depend on the same ratio, the steady-state concentrations of PAN and $O_3$ often exhibit a tight correlation, which has been widely used to examine the local $O_3$–PAN relationship.[56,58] PAN and $O_3$ thus tend to track one another temporally and geographically in photochemical smog.[59–61]

Peroxyacetyl radicals are generated from a broad set of hydrocarbons and their oxidation products, as shown in Fig. 1. PAN and PPN can be formed from precursors such as acetone, acetaldehyde, propionaldehyde, 2-butene, biacetyl, isoprene, and any aldehyde that yields acyl radicals upon OH attack, with nitric acid ($HNO_3$) formation acting as a competitive sink.[58] PAN-forming potentials have been quantified for several key

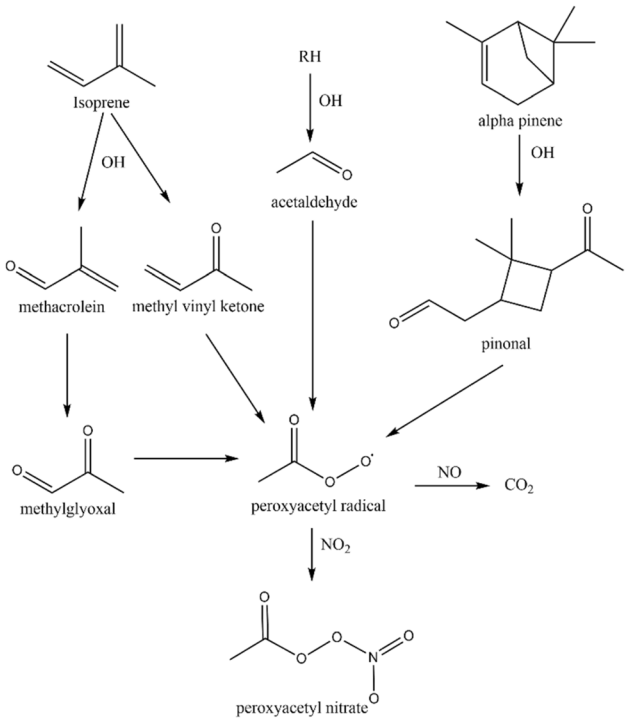


Fig. 1 VOC reactions to PAN formation.

hydrocarbons (*trans*-2-butene, propene, ethene, *n*-butane, and toluene) under conditions of 100 ppb $NO_2$, with reported PAN yields of ~50, 33, 6, and negligible linear yields for ethene and *n*-butane.[62] PAN formation generally follows OH reactivity trends of the parent hydrocarbons, since peroxyacetyl radicals originate from acetaldehyde or methylglyoxal.[62]

Despite its importance, PAN is not expected to photodissociate efficiently in the lower troposphere because it absorbs only weakly above ~290 nm.[56] It is also only moderately soluble in water and reacts slowly with OH, meaning that aqueous-phase scavenging and OH oxidation are relatively minor removal pathways.[27,56,63] PAN is nevertheless ubiquitous in the troposphere due to its efficient formation from common VOCs and $NO_x$ and its extended lifetime at cooler temperatures.

A nighttime source of PAN arises from nitrate radical ($NO_3$)-initiated oxidation of acetaldehyde:

$$CH_3CHO + NO_3 \rightarrow CH_3C(O)^{\bullet} + HNO_3$$

followed by rapid reaction of $CH_3C(O)^{\bullet}$ with $O_2$ or $NO_2$ to form peroxyacetyl radicals and ultimately PAN.[64] During the day, the analogous $CH_3CHO$ + OH pathway generates $CH_3C(O)^{\bullet}$, which undergoes the same sequence.[65] These $NO_3$ and OH-driven routes provide important nighttime and daytime sources of peroxyacetyl radicals that feed into the PAN reservoir.

**2.1.2 Removal mechanisms.** Outside of thermal decomposition, PAN loss occurs through a combination of heterogeneous processes, deposition, aqueous-phase reactions, and relatively slow gas-phase oxidation. PAN removal *via* OH is slow ($k < 3 \times 10^{-14}$ $cm^3$ per molecule per s at 298 K), and both wet and dry deposition processes are comparatively minor under

most conditions.[27,66] PAN deposition to surfaces is generally slow,[67,68] consistent with its modest water solubility and slow hydrolysis in aqueous solutions.[31] Measured dry-deposition velocities are ~0.25 cm $s^{-1}$ over soil and grass and ~0.01 cm $s^{-1}$ over water and ocean surfaces,[58] implying that deposition is a minor daytime sink but can become more important at night when mixing heights collapse and surface contact is enhanced.[69]

Marine and fog environments provide additional complexity. In fog events, observed decreases in PAN have been attributed to its thermal decomposition followed by uptake of peroxyacetyl radicals into fog droplets,[70] introducing a coupled gas–aqueous loss mechanism that may be particularly important in marine or coastal settings. At Arctic temperatures, however, thermal decomposition is not the only loss pathway; observations indicate additional sinks both at the surface and aloft, including heterogeneous and multiphase processes that are not yet fully constrained.[66,71]

The physical properties of PAN further shape its removal. PAN has a melting point of −48.5 °C and a boiling point of 104.5 °C, with vapor pressure described by:

$$\ln(P) = -\frac{4586}{T} + 19.04$$

where $P$ is in hPa and $T$ is in Kelvin.[58] PAN is essentially insoluble in water (Henry's coefficient ≈ 3.5 mol $L^{-1}$ $atm^{-1}$ at 22 °C) but is soluble in nonpolar organic solvents and hydrolyzes in basic solutions.[58,63,72] A parameterization of Henry's law constant:

$$H = 9.1 \times 10^{-11} \exp\left(-\frac{5400}{T}\right)$$

indicates a strong temperature dependence ($\Delta H_{sol}$ ≈ −54.2 kJ $mol^{-1}$),[69] but even at low temperatures, washout and rainout remain relatively inefficient removal processes compared to thermal decomposition.

Thermal decomposition is the dominant removal process for PAN in most of the troposphere and is responsible for its strong temperature sensitivity.[55] PAN decomposes *via* N–O bond homolysis to regenerate peroxyacetyl radicals and $NO_2$:

$$CH_3C(O)OONO_2 \rightarrow NO_2 + CH_3C(O)OO^{\bullet}$$

The peroxyacetyl radical can then react with NO, $HO_2$, or ($RO_2^{\bullet}$) to yield a variety of products, including $CH_3C(O)O^{\bullet}$, peroxides, acids, radicals, and $CO_2$.[55] The acetoxy radical ($CH_3C(O)O^{\bullet}$) is thermally unstable and can decompose to ($CH_3^{\bullet}$) and $CO_2$, further feeding radical chains. The local concentrations of NO and $NO_2$ thus not only control PAN formation but also influence the fate of its decomposition products. Because this radical pool regulates both $NO_x$ cycling and oxidant production, PAN decomposition directly alters local ozone chemistry and the $HO_x$/$RO_x$ balance, especially in polluted or NO-rich environments.

The thermal decomposition rate of PAN is both temperature- and pressure-dependent, and typical tropospheric conditions place PAN in the falloff regime of its unimolecular decomposition.[56] Over 280–330 K, the rate constant can be described by a Troe expression,[56] which combines low-pressure and high-pressure limits ($k_0$ and $k_\infty$) with a broadening factor $F = 0.3$. Using this parameterization, $k_\infty$ is ~$6.1 \times 10^{-4}$ $s^{-1}$ at 298 K, and the effective first-order rate constant for PAN decomposition at 298 K and 760 torr is ~$5.2 \times 10^{-4}$ $s^{-1}$, corresponding to a lifetime of ~30–50 minutes.[56] These values underline why PAN is short-lived in warm boundary layers but persists for long periods in cooler environments, creating strong vertical gradients and making PAN an efficient long-range $NO_x$ reservoir.

The temperature dependence of PAN decomposition can also be expressed in Arrhenius form over the tropospheric range:[26,34]

$$k_0(s^{-1}) = 1.58 \times 10^{16} e^{-112.5 \text{ kJ mol}^{-1}/RT}$$

which simplifies to[73]

$$k_0(s^{-1}) = 4.9 \times 10^{-3} e^{-12.1 \text{ kJ mol}^{-1}/T}[N_2]$$

At 298 K, this yields $k_0 \approx 3.3 \times 10^{-4}$ $s^{-1}$ and a PAN lifetime of ~50 minutes, consistent with experimental constraints.[26,34,73]

$$k_\infty(s^{-1}) = 5.4 \times 10^{16} e^{-13830 \text{ J mol}^{-1}/T}$$

The Troe falloff expression for PAN is as follows for the range of 280 K to 330 K:[56,74]

$$k = \frac{k_0[M]}{1 + k_0[M]/k_\infty} F^{\left\{1+\left(\frac{\log_{10} k_0[M]}{k_\infty}\right)^2\right\}^{-1}}$$

where $F$ is recommended to be 0.6,[74] slightly higher than the 0.3 used in earlier literature.[56]

PAN exists in a temperature- and $NO_x$-dependent equilibrium with its precursors (peroxyacetyl radicals and $NO_2$).[56] At night, decomposition of PAN in an environment with relatively high NO (≈10 ppb) can drive conversion of NO to $NO_2$ while generating HCHO *via* subsequent $CH_3O$ oxidation,[56] potentially maintaining a reservoir of photochemically active species that become important at sunrise:

$$CH_3O + O_2 \rightarrow HCHO + HO_2$$

This nighttime radical production pathway highlights that PAN decomposition is not simply a sink but a source of chemically active carbonyls and $HO_2$, enabling early-morning radical buildup once photolysis begins.

In the upper troposphere, where temperatures are typically lower than the bottom of the troposphere, thermal decomposition alone can give PAN lifetimes of days-to-months, as seen in Fig. 2. Under these conditions, photolysis and OH oxidation must be included to accurately represent PAN loss,[27,34] as seen in Fig. 3, which compares loss mechanisms for PAN in the atmosphere. Because both thermal decay and pressure-dependent kinetics

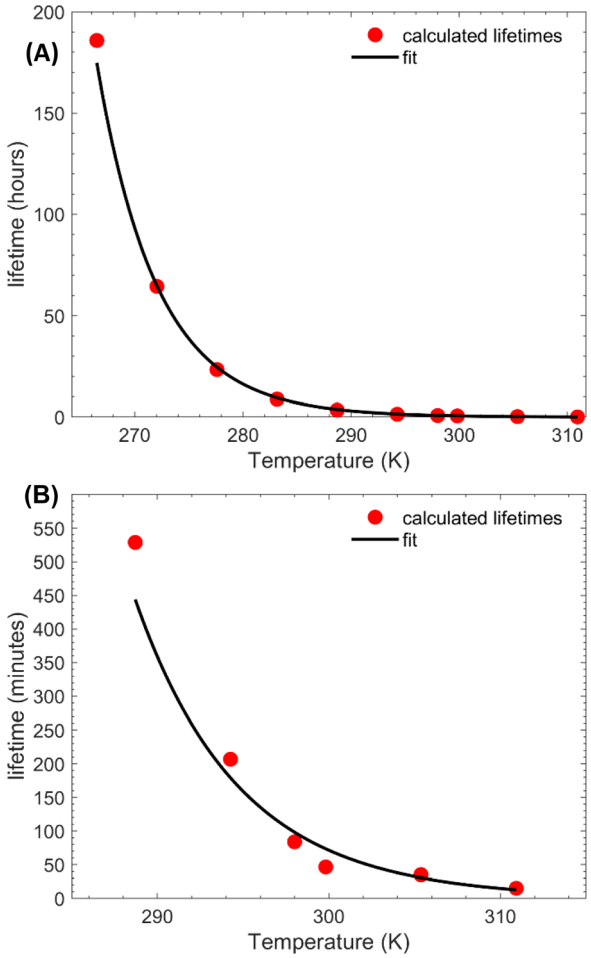


Fig. 2 Plot of calculated temperature-dependent lifetime of PAN: (A) overview from 264–311 K; (B) zoomed in view from 289 to 311 K.

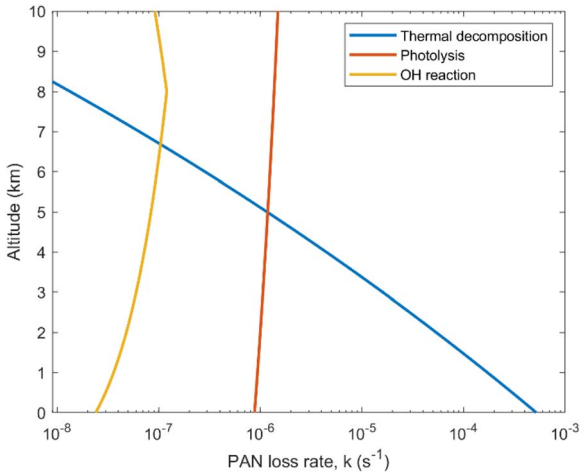


Fig. 3 Atmospheric loss processes of PAN as a function of altitude, following the framework of Talukdar *et al.* (1995).[27] PAN thermal decomposition was computed using JPL Chemical Kinetics and Photochemical Data Evaluation[75] rate expressions, while photolysis rates were derived from actinic flux fields generated by the NCAR TUV model (version 5.3).[76] Loss due to reaction with OH was calculated using U.S. Standard Atmosphere temperatures and a fixed OH concentration, consistent with the original Talukdar approach. Adapted from Talukdar *et al.* (1995)[27] with permission from Wiley R. K. Talukdar, J. B. Burkholder, A. M. Schmoltner, J. M. Roberts, R. R. Wilson and A. R. Ravishankara, Investigation of the Loss Processes for Peroxyacetyl Nitrate in the Atmosphere – UV Photolysis and Reaction with OH, *Journal of Geophysical Research-Atmospheres*, 1995, **100**, 14163–14173, copyright 2026.

slow dramatically with altitude, PAN becomes increasingly photolabile aloft, shifting its dominant loss mechanism from thermal decomposition to UV-driven processes above ~5–7 km.

Overall, the strong Arrhenius behavior of PAN decomposition explains its characteristic vertical structure, its sensitivity to synoptic temperature changes, and its ability to redistribute $NO_x$ over regional to hemispheric scales. Thermal decomposition thus underpins nearly all aspects of PAN's atmospheric role, from local oxidant chemistry in warm boundary layers to long-range $NO_y$ transport in the free troposphere.

Photolysis becomes an increasingly important PAN loss process at higher altitudes where actinic flux is strong and temperatures are low.[34] Early work by Aikin *et al.*[11] proposed a primary photolysis channel for PAN at 298 K:

$$PAN + h\nu \rightarrow CH_3C(O)OO + NO_2 + O^3P \ \lambda = 990 \pm 240 \text{ nm}$$

Subsequent work by Mazely *et al.*[1] suggested that lower threshold energies may allow significant internal energy partitioning into the products. If $NO_2$ is produced with sufficient internal excitation, secondary dissociation can occur:

$$PAN + h\nu \rightarrow CH_3C(O)OO + NO + O^3P \ \lambda = 281 \pm 35 \text{ nm}$$

$$PAN + h\nu \rightarrow CH_3C(O)OO + NO + O^1D \ \lambda = 195 \pm 15 \text{ nm}$$

These channels can lead, through subsequent radical chemistry, to reformation of PAN, making photolysis both a source and a sink in different parts of the chemical system.[66]

Mazely *et al.*[1] also proposed additional direct dissociation pathways, including:

$$PAN + h\nu \rightarrow CH_3C(O)O + NO_3 \ \lambda = 1025 \pm 215 \text{ nm}$$

Given the instability of the acetoxy radical, this channel yields an effectively irreversible loss of PAN.[66] $NO_3$ produced in this way is itself readily photolyzed to NO or $NO_2$ by visible light, returning $NO_x$ to the gas phase and releasing nitrogen that was previously sequestered in PAN.

Additional secondary dissociation channels of $NO_3^-$ were identified:[1]

$$PAN + h\nu \rightarrow CH_3C(O)O + NO_2 + O^3P \ \lambda = 375 \pm 30 \text{ nm}$$

$$PAN + h\nu \rightarrow CH_3C(O)O + NO_2 + O^1D \ \lambda = 235 \pm 10 \text{ nm}$$

and a suite of concerted, exothermic reactions involving bond rearrangement and cleavage, such as:[1]

$$PAN + h\nu \rightarrow CH_3 + CO_2 + NO_3 \ \lambda = 1395 \pm 340 \text{ nm}$$

$$PAN + h\nu \rightarrow CH_3 + CO_2 + NO_2 + O^3P \ \lambda = 415 \pm 30 \text{ nm}$$

$$PAN + h\nu \rightarrow CH_3 + CO_2 + NO_2 + O^1D \ \lambda = 250 \pm 10 \text{ nm}$$

$$PAN + h\nu \rightarrow CH_3C(O)O + O_2 + NO_2 \ \lambda = 445 \pm 35 \text{ nm}$$

$$PAN + h\nu \rightarrow CH_3C(O)O + O_2 + NO + O^3P \ \lambda = 209 \pm 10 \text{ nm}$$

$$PAN + h\nu \rightarrow CH_3C(O)O + O_2 + NO + O^1D \ \lambda = 157 \pm 3 \text{ nm}$$

At 298 K, Mazely *et al.*[1] proposed two particularly important exothermic channels:

$$PAN + h\nu \rightarrow CH_3O + CO_2 + NO_2 \ \Delta H_{rxn} = -20 \pm 5 \text{ kcal mol}^{-1}$$

$$PAN + h\nu \rightarrow CH_3O_2 + CO_2 + NO \ \Delta H_{rxn} = -6 \pm 5 \text{ kcal mol}^{-1}$$

The uncertainties in these energetics arise from the experimental heats of formation of $CH_3C(O)O$, $CH_3C(O)O_2$, and PAN.[1]

From a practical standpoint, PAN photolysis in the atmosphere is often summarized in terms of three main pathways with thresholds near 1025, 990, and 445 nm,[34] corresponding broadly to $NO_3$ + $CH_3C(O)OO^{\bullet}$, $NO_2$ + $CH_3C(O)OO^{\bullet}$, and $NO_2$ + $O_2$ + $CH_3C(O)$ products.[34] Quantum yields for $NO_2$ and $NO_3$ formation are wavelength dependent. Mazely *et al.*[1,77] reported $\phi(NO_2) = 0.83 \pm 0.09$ and $\phi(NO_3) = 0.30 \pm 0.10$ at 248 nm using $N_2O_5$ photolysis as a reference. A later study revised $\phi(NO_3)$ to $0.19 \pm 0.04$ after correcting the assumed $N_2O_5$ quantum yield, but still found good agreement with Mazely *et al.*[78] Harwood obtained $\phi(NO_3) = 0.41 \pm 0.10$ at 308 nm, again indicating strong wavelength dependence. Flowers *et al.*[66] reported $\phi(NO_3) = 0.31 \pm 0.08$ at 289 nm, and later work extending from 289–308 nm and at 312 nm found $\phi(NO_3) = 0.30 \pm 0.07$ and $0.39 \pm 0.07$, respectively.[79]

Taken together, these results show that PAN photolysis is spectrally complex and yields multiple channels that either recycle PAN precursors or irreversibly return $NO_x$ to the atmosphere. Although photolysis is a minor sink in the boundary layer compared to thermal decomposition, it becomes increasingly important above ~5 km altitude, where low temperatures slow thermal decay and allow PAN to act as a photolabile $NO_x$ reservoir.[27,34,80]

### 2.2 Lifetime in the atmosphere

The atmospheric lifetime of PAN is strongly controlled by ambient temperature and the local $NO_2$/NO ratio.[81] At temperatures above 273 K, PAN lifetimes are typically on the order of hours,[82] while in the cold upper troposphere, lifetimes can extend to months.[14] Zhang *et al.*[83] reported an extreme temperature dependence, with a PAN lifetime of 5.36 years at 247 K and only ~30 minutes at 298 K. PAN is also long-lived with respect to oxidation by OH (≈1 year at $[OH] = 1 \times 10^6$ molecule per $cm^3$) and with respect to photolysis in the boundary layer (≈30 days),[27,80] confirming that thermal decomposition dominates its removal in most of the lower troposphere.

When photolysis alone is considered, the *e*-folding (1/*e*) lifetime of PAN is on the order of ~3 months, whereas reaction with OH proceeds with $k \leq 3 \times 10^{-14}$ $cm^3$ per molecule per s and represents only a minor loss pathway.[58] Thus, in the lower and mid-troposphere, PAN's effective lifetime is set primarily by temperature-dependent thermal decay. In contrast, at higher altitudes where temperatures are low and actinic flux is strong, PAN can persist long enough that photolysis and reaction with OH become competitive with thermal decomposition.[27,34,80] Overall, PAN's lifetime spans from tens of minutes in a warm polluted boundary layer to months in the cold upper troposphere, which underpins its role as a long-range $NO_y$ reservoir.[14,27,34,80,83]

## 3 Atmospheric sources

While Section 2 describes PAN chemistry from a mechanistic perspective independent of emission context, this section focuses on real-world precursor sources and transport processes that control PAN variability.

PAN is not emitted directly into the atmosphere; instead, it is produced secondarily through the photochemical oxidation of volatile organic compounds (VOCs) in the presence of $NO_x$. As such, it is a secondary pollutant. Its atmospheric abundance therefore reflects a combination of *in situ* formation, precursor availability, temperature, and large-scale transport.

### 3.1 *In-situ* formation

PAN formation begins with the production of peroxyacetyl (PA) radicals during VOC oxidation. Anthropogenic carbonyls and aromatics are major contributors in polluted environments, supplying a substantial fraction of the PA radical pool.[84] Quantitative apportionment studies show that carbonyls contribute roughly 59% of PAN formation, with aromatics supplying ~26% and biogenic VOCs contributing ~10%.[6] These results emphasize the strong coupling between urban VOC emissions and PAN production, especially during summertime pollution episodes when photochemical activity is high.[40]

Biogenic VOCs also play a substantial role. Isoprene oxidation produces a family of peroxyacyl nitrates that serve as source-specific tracers of biogenic chemistry.[84] Oxidation of methacrolein and methyl vinyl ketone further contributes to the PA radical pool.[9] Although biogenic precursors typically constitute a smaller fraction of PAN formation than anthropogenic carbonyls, they dominate in forested regions and during periods of high isoprene emissions.[7]

Biomass burning and wildfires represent major episodic sources of PAN. Observations in African biomass-burning plumes show strong enhancements in both PAN and PAA, with PAN/PAA ratios evolving systematically as plumes age.[31] Similar PAN enhancements have been reported in forest-fire outflow.[32,85] Because PAN is thermally unstable, it decays more rapidly than PAA, making the PAN/PAA ratio a useful indicator of plume age and transport history.[54] Cold, lofted plumes in the free troposphere allow PAN to persist longer, enabling it to be transported over large distances.[31,32]

PAN can also increase during severe haze events. Under stagnant wintertime or summertime haze conditions, elevated radical production on aerosol surfaces, enhanced oxidation of carbonyl precursors, and limited boundary-layer mixing can all contribute to locally elevated PAN.[6,40] These environments highlight the nonlinearity of PAN chemistry and its sensitivity to both VOC composition and atmospheric stagnation.

### 3.2 Transport and non-local sources

Because PAN is thermally stable at low temperatures, it often accumulates in the free troposphere, where it can comprise a large fraction of $NO_y$. Long-range transport is therefore a dominant source of PAN for many regions. Trans-Pacific and intercontinental transport events frequently deliver PAN-rich air masses, with some studies showing ~21% increases in PAN during strong outflow episodes and PAN comprising ~70% of $NO_y$.[36,86] Similar signatures appear in Siberian biomass-burning outflow and African fire plumes that have been lofted into the free troposphere.[31,32,86]

PAN also plays an important role in the UTLS. Cold UTLS temperatures greatly extend PAN's lifetime, allowing it to act as an efficient carrier of $NO_x$.[59] PAN has been observed in aircraft corridors and upper-tropospheric flight tracks,[58] and both lightning-produced $NO_y$[87] and stratosphere–troposphere exchange events[37,57] contribute to enhanced PAN aloft.

Strong spatial and seasonal patterns further reflect these transport influences. Northern Hemisphere PAN levels exceed those of the Southern Hemisphere due to larger anthropogenic VOC and $NO_x$ emissions[7] and more frequent wildfire activity.[32,85] High-elevation sites such as Jungfraujoch, Mauna Loa, Mt. Bachelor, and locations downwind of Los Angeles often exhibit elevated PAN linked to upslope flows and subsidence of free-tropospheric air.[36,86] Seasonal maxima commonly occur in spring and fall, when moderate temperatures and sufficient actinic flux favor PAN stability and formation, while winter suppression reflects limited photochemistry and summer suppression often reflects rapid thermal loss.[40]

## 4 Measurement techniques

PAN presents persistent analytical challenges due to its thermal instability, tendency to decompose on surfaces, and moderate solubility in water.[58] These properties shape nearly all measurement techniques and often influence instrument design as much as the detection scheme itself. Historically, gas chromatography (GC), particularly GC coupled with electron capture detection (GC-ECD), provided the foundation for PAN measurements. However, modern thermal-dissociation (TD) methods paired with chemiluminescence, optical spectroscopy, or mass spectrometry now offer substantially higher time resolution, reduced sampling artifacts, and improved selectivity. PAN measurement approaches can therefore be broadly categorized into chromatographic, thermal dissociation-based, spectroscopic, and mass spectrometric techniques, each involving trade-offs between sensitivity, temporal resolution, and susceptibility to interferences. The following subsections synthesize the principles, performance characteristics, and limitations of the major techniques used to quantify PAN in the atmosphere.

### 4.1 Calibration and synthesis techniques

PAN poses hazards in laboratory settings. Stephens *et al.* (1969) documented explosive accidents during PAN handling,[88] noting that liquid PAN is unsafe under pressure and that cold storage can lead to condensation and detonation. Recommendations include handling PAN primarily in vapor form diluted with inert gases, maintaining storage temperatures above 10 °C, avoiding pressurization, and using machined rather than cast fittings. PAN vapor itself does not appear to pose a significant explosion risk, but condensed PAN does. In one documented event, decomposition produced carbon monoxide, carbon dioxide, formic acid, methyl nitrite, and nitrogen dioxide after the explosion.[88]

The synthesis of PAN standards has historically been one of the main limitations for accurate quantitative measurements, since early preparation methods produced unstable mixtures that required extensive purification.[58] The first laboratory syntheses relied on the photolysis of alkyl nitrites in the presence of oxygen, which generates PAN through the reaction

$$C_2H_5ONO + 2O_2 + h\nu \rightarrow CH_3C(O)OONO_2 + H_2O.$$

Although effective, this approach produced numerous byproducts that made routine calibration difficult.

Later methods focused on stabilizing PAN in a nonvolatile liquid matrix at low temperatures.[58] In this approach, PAN is produced by nitrating peracetic acid and storing the resulting mixture at −78 °C, where it remains stable for several weeks. The mixture can then be introduced into a capillary diffusion tube held at 0 °C. Air flowing over the tube produces gas-phase PAN concentrations from 1 to 50 ppb after removing residual nitric acid with a nylon filter. This technique enabled more consistent calibration sources.

Liquid PAN is extremely explosive at room temperature,[89] but several protocols have been developed to allow safer handling and storage. Nielsen *et al.*[89] generated PAN in *n*-heptane at 0 °C using 1.2 M peracetic acid and sulfuric acid. After reaction, the mixture was poured over ice water and the organic phase was separated, yielding PAN dissolved in heptane. Gaffney *et al.*[90] improved the stability of the product by substituting *n*-tridecane for heptane, which reduced volatility and lowered the associated risk.

A number of gas-phase photochemical routes have also been used to generate PAN for laboratory calibrations. Photolysis of acetaldehyde in the presence of NO in a flow reactor produces PAN reproducibly.[91] PAN can also be generated from acetone, excess NO, $O_2$, and UV light,[92–95] following the established radical sequence:

$$CH_3C(O)CH_3 + 2O_2 \rightarrow CH_3(O)OO + CH_3OO$$

$$CH_3(O)OO + NO \rightarrow CH_3C(O)O + NO_2$$

$$CH_3OO + NO \rightarrow CH_3 + NO_2$$

$$CH_3C(O)OO + NO_2 \rightarrow CH_3C(O)OONO_2$$

A minor channel (<6%) produces methyl nitrate from reactions involving $CH_3$ radicals and $NO_2$.[95] Batch synthesis of PAN is prone to thermal decay, so continuous flow reactors remain the preferred approach for maintaining a stable output over extended periods.

Additional liquid-phase pathways have been developed, including reaction of $H_2O_2$ with acetic acid followed by nitration with $HNO_3$ in the presence of $H_2SO_4$ and tridecane at 0 °C.[96] Other laboratory routes include ethyl nitrite photolysis in a dynamic gas reactor followed by GC purification,[69] $Cl_2$-initiated acetaldehyde photolysis,[69] and acetone photolysis at 254 nm.[69] Together, these methods provide a range of practical options for producing PAN depending on the needs of the experiment and required stability of the standard.

### 4.2 Gas chromatography (GC)

**4.2.1 GC with electron capture detection (GC-ECD).** Gas chromatographic techniques provide high chemical specificity and historically enabled the first routine PAN observations, but they are limited by relatively long analysis times and potential sampling losses. Reported GC-ECD detection limits typically range from ~1–50 pptv depending on sampling configuration, analytical cycle time, and the use of preconcentration strategies, with longer integration times generally yielding the lowest detection limits.[55,57,58,70,85,91,97–106] Under optimized laboratory and field conditions, sub-ppt sensitivity has been demonstrated, although performance in routine deployments is more commonly constrained by sampling artifacts and chromatographic cycle duration.

Campaign and field deployments have also demonstrated the robustness of GC-ECD. Field studies in remote and upper-tropospheric environments demonstrate that automated GC-ECD systems can achieve low-ppt detection limits and maintain stable performance under challenging sampling conditions, including polar and airborne deployments.[107–109]

Cryogenic preconcentration is frequently integrated with GC-ECD. Cryotrapping and related preconcentration approaches can further enhance sensitivity and are widely used in low-concentration environments such as the remote troposphere.[110,111] However, cryosampling introduces known sampling artifacts: several studies[62,112,113] have documented 10–20% PAN loss during cryogenic concentration. These losses require explicit correction, especially in the remote troposphere where PAN concentrations are low and residence times in sampling lines are long.

**4.2.2 GC with alternative detectors.** In addition to ECD, several alternative GC detection schemes have been applied to PAN with varying degrees of success. Chemiluminescence-based GC approaches provide improved temporal resolution relative to conventional GC-ECD systems, typically achieving sub-ppbv detection limits with acquisition times of seconds to minutes depending on the configuration.[114–117] Pulse-discharge detectors offer high sensitivity and good analytical precision, although their deployment remains comparatively limited in field studies.[92] Coupling GC separation with negative-ion chemical ionization mass spectrometry provides enhanced molecular specificity and improved selectivity for PAN relative to traditional detector configurations, albeit with longer analytical cycle times and increased instrumental complexity.[118]

Preconcentration strategies such as charcoal sorbent trapping remain essential for achieving low detection limits and facilitating intercomparison between GC-ECD and alternative detection approaches.[119,120] Hybrid configurations combining GC separation with cryogenic trapping and $NO_y$ chemiluminescence detection can achieve sub-ppt sensitivity under optimized conditions, although these systems conceptually overlap with thermal-dissociation approaches and are therefore less commonly used as standalone GC methods.[121]

### 4.3 Thermal dissociation approaches

Thermal dissociation techniques allow near-real-time PAN measurements but require careful inlet temperature control to avoid interferences from other $NO_y$ species. TD techniques decompose PAN into $NO_2$ or peroxyacetyl radicals in a heated inlet prior to detection. Because thermal decomposition is rapid relative to detection timescales, TD methods enable high-frequency, near-real-time PAN measurements and have become central to modern field campaigns.

**4.3.1 Luminol-based chemiluminescence.** Thermal dissociation followed by chemiluminescent $NO_2$ detection represents one of the earliest real-time PAN measurement strategies. These systems provide moderate sensitivity and robust field performance but require careful inlet temperature control to prevent interferences from other thermally labile $NO_y$ species.[122] Hybrid configurations incorporating cryogenic preconcentration or optical detection have achieved sub-ppt sensitivity under optimized conditions.[61,121]

**4.3.2 Thermal dissociation cavity ring-down spectroscopy (TD-CRDS).** TD-CRDS systems combine thermal conversion of PAN to $NO_2$ with highly sensitive optical detection, enabling fast time response and low-ppt detection limits. These instruments typically employ dual-channel configurations to separate thermally generated $NO_2$ from ambient backgrounds. Performance is influenced by optical interferences (*e.g.*, $O_3$, $H_2O$, and NO) and requires careful calibration of thermal dissociation efficiency and spectroscopic corrections.[96,123] Non-thermal CRDS systems are discussed separately in Section 4.3.2.

**4.3.3 Thermal dissociation chemical ionization mass spectrometry (TD-CIMS).** TD-CIMS provides some of the highest sensitivities currently achievable for PAN detection, with low-ppt detection limits and sub-second time resolution in optimized configurations. These systems rely on thermal conversion of PAN to reactive radicals followed by ion–molecule detection, offering strong molecular specificity but requiring careful control of interferences such as peroxyacetic acid (PAA), humidity effects, and ion chemistry perturbations.[96,124–127] Airborne implementations further demonstrate the versatility

of TD-CIMS for upper-tropospheric and remote-environment measurements, although instrument complexity and calibration requirements can limit routine deployment.[128]

**4.3.4 Thermal dissociation laser-induced fluorescence (TD-LIF).** TD-LIF approaches provide rapid time response and the ability to differentiate multiple $NO_y$ species through temperature-resolved dissociation schemes. These systems typically achieve sub-ppbv detection limits with high temporal resolution, although performance depends strongly on inlet temperature control and fluorescence calibration stability.[129–131]

### 4.4 Spectroscopic analysis

Optical spectroscopic approaches offer calibration stability and minimal sampling artifacts but typically have higher detection limits and greater susceptibility to spectral interference.

**4.4.1 Fourier transform infrared spectroscopy (FTIR).** FTIR detection of PAN exploits characteristic mid-infrared absorption features and provides high chemical specificity with excellent calibration stability. Detection limits vary widely depending on the optical pathlength and retrieval approach, ranging from laboratory sub-ppb sensitivities to multi-ppb limits in atmospheric applications.[3,4,84,132,133] Airborne and remote-sensing FTIR platforms provide important constraints on PAN vertical distributions, although uncertainties remain larger than for *in situ* techniques.[35,61]

**4.4.2 Cavity ring-down spectroscopy (CRDS).** Non-thermal CRDS implementations enable optical detection of PAN-related species with fast temporal resolution and moderate sensitivity. These approaches benefit from stable spectroscopic baselines but require careful correction for overlapping absorbers and calibration against $NO_2$ standards.[134]

**4.4.3 Satellite-based PAN retrievals.** Satellite observations provide global constraints on PAN distributions using thermal-infrared retrievals, enabling analysis of long-range transport, biomass-burning impacts, and upper-tropospheric nitrogen chemistry. Current satellite products achieve sub-ppbv sensitivity with uncertainties typically larger than those of *in situ* measurements but provide uniquely valuable spatial coverage[69,135–137]

**4.4.4 Defined absorption cross-sections.** Accurate absorption cross-sections underpin all spectroscopic PAN measurement techniques. Laboratory and theoretical studies collectively define PAN absorption behavior across the UV-vis and IR regions, forming the basis for both remote-sensing retrievals and *in situ* optical detection.[1,14,138] These data form the basis of the HITRAN[139] PAN dataset, which incorporates results from several laboratory sources[140,141] to generate a composite IR spectrum across the full 550–2200 $cm^{-1}$ region (Fig. 4). Additional UV-vis cross-sections are available through the MPI-Mainz UV-vis spectral atlas of gaseous molecules of atmospheric interest,[142] which includes fourteen published spectra[27,143–149] covering the 200–350 nm range (Fig. 5). Absorption cross-sections for acetylperoxy radicals have also been defined[12] (Fig. 6). Together, these datasets establish a reliable set of cross-sections for PAN and allow analysis of both its photolysis and thermal behavior across relevant atmospheric wavelengths.

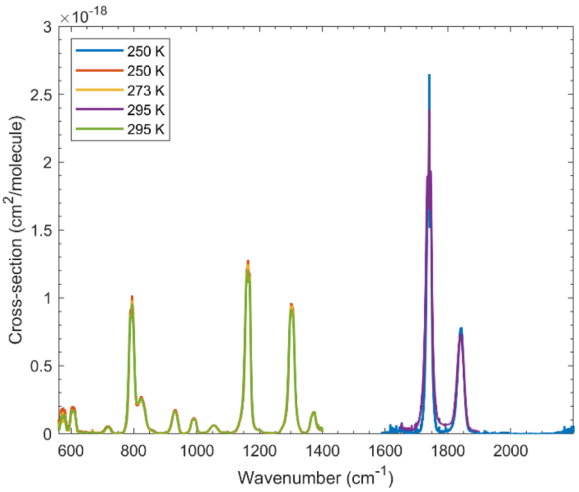


Fig. 4 HITRAN IR spectrum of PAN at multiple temperatures.[139]

### 4.5 Derivatization and conversion methods

Derivatization and conversion approaches provide alternative strategies for PAN quantification but are used less frequently due to limited time resolution and potential selectivity challenges relative to thermal-dissociation and optical techniques.[150]

### 4.6 Mass spectrometry (MS)

Direct mass-spectrometric detection of PAN offers high chemical specificity and fast temporal response but generally requires complex calibration strategies and careful control of ion–molecule chemistry.

**4.6.1 Chemical ionization atmospheric pressure interface time-of-flight mass spectrometry (CI-APi-TOF-MS).** CI-APi-TOF-MS enables simultaneous detection of multiple peroxyacyl nitrates with high sensitivity and rapid acquisition rates, making it well suited for process studies and chemical-mechanism evaluation.

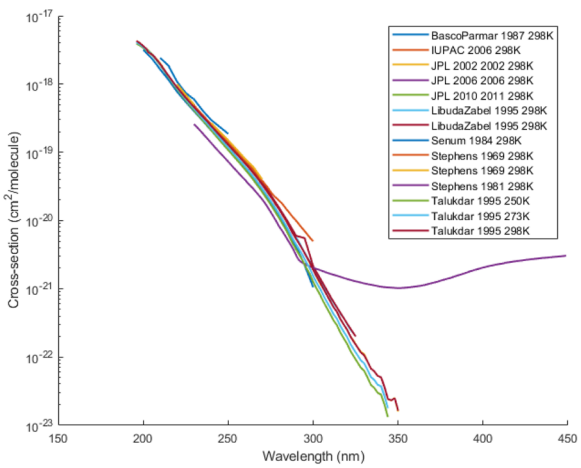


Fig. 5 UV-vis spectra of PAN found in the MPI-Mainz UV-vis spectral atlas of gaseous molecules of atmospheric interest.[27,142–149]

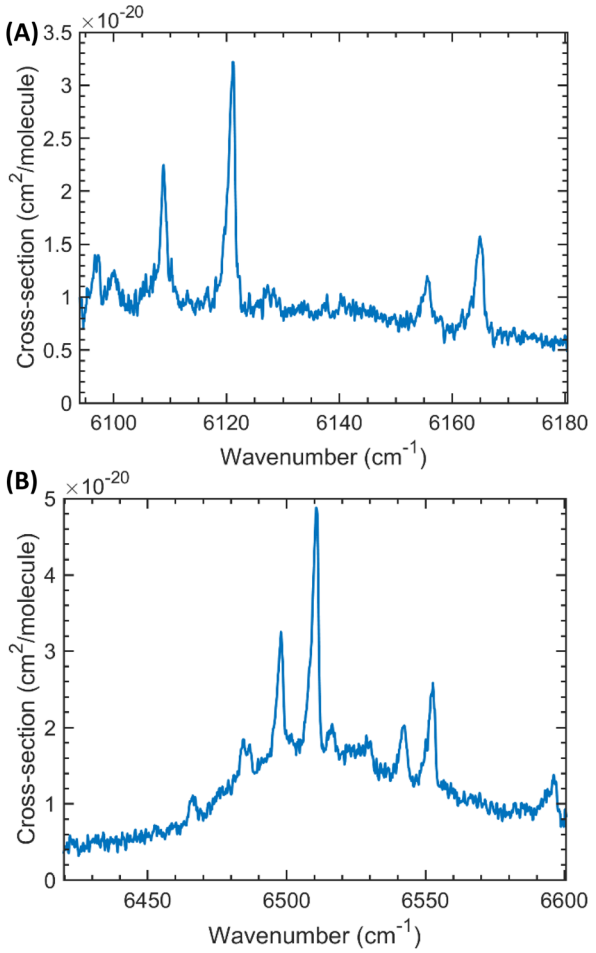


Fig. 6 IR spectra of acetylperoxy radicals[12] in two regions: (A) 6100–6170 $cm^{-1}$ and (B) 6450–6600 $cm^{-1}$.

**4.6.2 Selected-ion flow drift tube proton transfer mass spectrometery (SIFDT-PTR-MS).** PTR-based approaches such as SIFDT-PTR-MS provide near-real-time detection of PAN with moderate sensitivity and are particularly useful in dynamic environments where rapid concentration changes occur.[151]

# 5 PAN modelling

Modeling studies of peroxyacetyl nitrate (PAN) span laboratory chamber mechanisms, observation-constrained box models, regional chemical transport models, and global Earth-system simulations. Together, these modeling efforts illustrate PAN's dual role as both a diagnostic indicator of photochemical processing and a key $NO_x$ reservoir that shapes downwind $O_3$ formation, oxidant cycling, and long-range reactive nitrogen export.

## 5.1 Early modeling and mechanistic development

The first generation of PAN modeling focused on validating chemical mechanisms against chamber observations during the 1970–1980s. Classic studies such as those by Dunker *et al.* developed some of the earliest PAN isopleths, which compared predicted PAN sensitivities in different chemical mechanisms and showed strong model-to-model variability in PA radical production and $NO_2$ availability.[152] These early studies established that PAN, like $O_3$, exhibits strongly nonlinear dependence on the VOC/$NO_x$ ratio, laying the foundation for modern sensitivity analyses.

## 5.2 Observation-based and box-model studies

Observation-constrained box models have provided key insight into PAN formation pathways and model performance in diverse environments. For example, a Photochemical Box Model coupled with the Master Chemical Mechanism (PBM-MCM) has historically underestimated PAN.[85] This underestimate was traced to insufficient treatment of regional transport,[85] highlighting PAN's ability to accumulate upwind of the measurement site and be imported into the local photochemical system. Box-model studies have also quantified the contributions of different VOC classes to PAN production: carbonyls contribute ~59%, aromatics ~26%, and biogenic VOCs ~10%.[85] These same models quantify how PAN formation suppresses $HO_x$ and $NO_2$ while increasing NO, resulting in reduced $O_3$ formation rates, which are estimated at 2.84 ppb $O_3$ suppressed per 1 ppb PAN formed, with overall $O_3$ production slowed by ~36%.[85]

Other observation-based studies further show that PAN and $O_3$ are tightly correlated in both time and space,[61] allowing PAN to serve as a proxy for regional background $O_3$ (ref. 41) and as a more reliable indicator of photochemical smog than $O_3$ itself.[42,43]

## 5.3 Regional and global chemical transport modeling

Large-scale regional and global modeling has further clarified PAN's importance as a $NO_x$ reservoir and long-range transport agent. At low temperatures, PAN can account for 50–90% of $NO_y$ in the troposphere[33,34] and ~30% of $NO_y$ near 10 km altitude.[35] Global models show that 11–30% of total $NO_y$ originates from PAN decomposition,[153] confirming its major role in remote $NO_x$ budgets. Sensitivity analyses indicate that PAN greatly enhances $O_3$ formation in the remote northeastern Pacific by releasing $NO_x$ upon thermal decomposition; this enhancement varies with synoptic transport patterns.[153]

Models also show that megacities are exporters of PAN, which transports $NO_x$ reservoir capacity far downwind, enabling $O_3$ formation distant from the source region.[54,86] Climate-driven changes in temperature, radiation, precipitation, and wind speed have already contributed to a global decline in PAN,[154] something now resolved in several global simulations.

## 5.4 Chambe studies and model evaluation

Early smog-chamber investigations established the mechanistic sensitivity of PAN formation to hydrocarbon–$NO_x$ chemistry and now form the foundation for modern chemical transport and box models, which incorporate updated VOC oxidation schemes, multiphase chemistry, and detailed peroxyacyl nitrate formation pathways.[16,17,51,52] As a result, chamber-derived PAN sensitivities continue to serve as critical benchmarks for evaluating model performance across chemical regimes.

Large-scale chamber-experiments have provided important mechanistic insights into how PAN influences photochemical smog formation. A 5800 L Teflon chamber at the Statewide Air Pollution Research Center (University of California, Riverside) was used to conduct controlled simulations at 300 K.[16,155] These studies demonstrated that the presence of PAN significantly enhances smog production. PAN decomposition in the presence of NO generates peroxyacetyl and $NO_2$, increasing radical levels and accelerating $O_3$ formation. Systems containing PAN showed faster hydrocarbon consumption, higher $O_3$ production rates, and larger peak $O_3$ concentrations. The experiments also suggested that PAN carried over from a previous pollution episode can increase $O_3$ levels on the following day by providing an early-morning source of $NO_2$ and radicals. In the absence of sunlight, PAN was also found to react with NO to produce additional $NO_2$, which can further influence early photochemistry.

A related set of 249 outdoor smog-chamber experiments examined the formation of PAN and nitric acid in the Los Angeles Basin.[17,156] Eight chambers located at two Los Angeles sites were filled with morning ambient air, after which NMHC and $NO_x$ levels were systematically adjusted to simulate different chemical regimes relative to a control. The results were used to construct PAN isopleths (HC *versus* $NO_x$). Reductions in hydrocarbons, $NO_x$, or both resulted in lower PAN concentrations, while only $NO_x$ reductions led to substantial decreases in $HNO_3$. However, decreasing $NO_x$ also increased $O_3$ levels due to reduced titration, which required proportionally larger hydrocarbon reductions to counteract the increase. These chamber results highlight the nonlinear response of both PAN and $O_3$ to precursor emissions and illustrate the need to consider PAN chemistry when evaluating $O_3$ strategies. Subsequent chamber studies have extended these findings to other peroxyacyl nitrates, including MPAN formed during isoprene oxidation, demonstrating similar nonlinear sensitivity to $NO_x$–VOC regimes and providing constraints on secondary organic aerosol formation pathways.

### 5.5 PAN isopleths in modern modeling

PAN isopleths have re-emerged in modern air-quality studies. Recent efforts in China have used observation-based modeling to generate net-PAN-production isopleths, showing that PAN formation is overwhelmingly VOC-limited, not $NO_x$-limited.[157,158] These studies demonstrate that emission controls targeting $O_3$ generally also suppress PAN, and that PAN isopleths have broadly similar shapes to $O_3$ isopleths, simply shifted toward higher VOC/$NO_x$ ratios.[157,158] Global modeling work has applied PAN isopleths to study vertical gradients and long-range transport, showing distinct PAN–$O_3$ relationships across the troposphere.[159]

Fuel composition can also influence PAN. Ethanol–gasoline blends can increase peroxyacetyl radical and PAN production in winter.[160,161] The PAN-to-$O_3$ relative production ratio (RPR) introduced by Sun *et al.* (2020) varies with precursor levels and is highest under VOC-rich, $NO_x$-poor conditions.[162] PAN exhibits strong source signatures: MPAN indicates biogenic sources, whereas peroxypropionyl nitrate (PPN) correlates with anthropogenic emissions.[163–165]

### 5.6 PAN, SOA chemistry, and multiphase interactions in models

Modeling studies increasingly incorporate multiphase chemistry affecting the broader peroxyacyl nitrate family. The MPAN–isoprene pathway is explicitly represented in modern mechanisms, with MPAN oxidation leading to low-volatility organic acids, methacrylic acid epoxide (MAE), and related species that significantly contribute to SOA formation even though MPAN itself is not a nucleating vapor.[166,167] Heterogeneous processing of PAN on real-world $PM_{2.5}$ has been observed and is modeled as a minor but non-negligible loss pathway that produces particulate nitrate and oxidized organic fragments.[168] Co-variability between PAN and $PM_{2.5}$ across haze events confirms shared precursors and coupled oxidation dynamics,[169,170] and models increasingly treat PAN as both an oxidant reservoir and a proxy for multi-phase radical chemistry.

PAN also participates in multiphase chemistry linked to haze. Although PAN is not a primary nucleating species for secondary organic aerosols (SOAs) because it is too volatile and thermally unstable,[170] field studies consistently show that PAN correlates with elevated $PM_{2.5}$ and haze intensity.[169,170] Aerosol surfaces may promote additional PAN formation *via* heterogeneous radical sources, and PAN undergoes small but meaningful heterogeneous uptake producing particulate nitrate and oxidized fragments.[168] The broader PAN family also intersects with SOA pathways through peroxymethacryloyl nitrate to methacrylic acid epoxide (MPAN → MAE) chemistry.[166,167] PAN-like ions have been detected in 1–2 nm clusters by ion-cluster spectrometry, but the signals are weak and do not indicate PAN-driven nucleation.[171]

### 5.7 Emerging modeling areas

Several modeling areas have gained visibility recently:

1. Urban boundary-layer chemistry: modeling in Shenzhen confirms that PAN is strongly VOC-limited and contributes to midday $O_3$ peaks under high-temperature, stagnant conditions.[172]

2. Seasonal shifts: models explain observed spring and fall PAN maxima as arising from favorable combinations of temperature, photolysis rates, and carbonyl precursor availability.[59,60,110]

3. Fuel-change impacts: modeling shows that ethanol–gasoline blends increase PA radical production and raise PAN levels in winter.[160,161]

4. Aerosol–PAN interactions: mechanisms now include heterogeneous processing of PAN on PAH-rich particles.[54]

Together, these advancements show that modern PAN modeling now spans direct gas-phase chemistry, multi-phase interactions, photochemical regimes, and long-range transport—positioning PAN as one of the most important integrative species in atmospheric chemistry.

## 6 Measurement campaigns

Atmospheric measurements of PAN span more than six decades and now encompass urban centers, rural regions, marine

boundary layers, and polar environments. Because PAN is formed entirely *in situ* from VOC–$NO_2$ chemistry and exhibits strong temperature sensitivity, its abundance varies widely across locations and seasons. Long-term PAN records are uncommon, and most observational knowledge comes from targeted field campaigns with distinct chemical and meteorological contexts. The following subsections summarize major features of PAN variability in different environments and highlight characteristic ranges observed in each setting. Each section includes a map of where PAN has been measured in that type of environment (Fig. 7–12) with corresponding tables that list location, sampling period, mean concentration, maximum concentration, and altitude above sea level (Tables S1–S5).

### 6.1 Urban

Urban areas consistently exhibit the highest PAN concentrations due to abundant anthropogenic VOCs and $NO_x$ emissions that drive rapid photochemical formation. In Los Angeles, PAN historically exceeded 20–30 ppb during severe smog episodes,[173,207,249] with strong co-variation with ozone and a well-defined afternoon peak.[34] Modern megacities such as those in China continue to show large PAN burdens: autumn observations in the rural North China Plain, downwind of major urban centers, indicate that rapid PAN production can occur even under low-$NO_x$ conditions because HCHO photolysis and acetaldehyde oxidation substantially enhance peroxyacetyl radical formation.[57] Urban PAN formation often remains VOC-limited, and studies show that PAN can reduce net $O_3$ production by ~36% for each 1 ppb of PAN formed,[85] reflecting strong nonlinear sensitivity to precursor emissions. Although peak values have declined in some cities as $NO_x$ emissions have decreased,[154] urban regions still account for many of the highest PAN concentrations measured globally.

Because PAN is long-lived at cold temperatures, it is a major transport medium for $NO_y$ between atmospheric layers.[208] Long-range transport influences PAN throughout the western United States, with Siberian biomass burning and trans-Pacific transport producing ~21% PAN variability and strong springtime enhancements.[209] PAN is frequently elevated downwind of urban centers,[34] including mountain sites northeast of Los Angeles,[173,207] where concentrations have historically reached up to 35 ppb.[44,173,207] Seasonal and diurnal patterns reinforce its photochemical origin.[61]

Fig. 8 World map showing the locations where PAN has been measured in urban regions. Regions appear darker red the more extensively they have been studied.[42,43,59,61,99,101,110,111,116,125,150,163,165,173–206]

### 6.2 Rural

Rural PAN measurements frequently reveal the combined influence of transported pollution, biomass burning plumes, and biogenic VOC oxidation. PAN often maximizes in spring and fall,[59,60,110] reflecting seasonal changes in photochemistry, biomass burning, and long-range transport. In regions influenced by agricultural or forested landscapes, carbonyl compounds dominate PAN formation, and model analyses attribute ~59% of PAN production to carbonyl precursors, with aromatics and biogenic VOCs contributing the remainder.[85] Rural observations in Southeast China show strong daytime PAN maxima and correlations with $O_3$ and HCHO,[87] consistent with photochemically driven radical production. Episodic biomass-burning plumes can also dominate PAN variability in rural environments, particularly during boreal fire seasons and springtime long-range transport events. Rural measurements are also instrumental in diagnosing regime behavior: PAN isopleths, broadly similar in shape to $O_3$ isopleths, have long been used to distinguish VOC- *versus* $NO_x$-sensitive conditions.[152,157,159,250]

Observations demonstrate strong seasonal behavior: PAN often maximizes in fall and spring.[59,60,110] Coastal observations in Southeast China show spring/summer PAN peaks with strong midday maxima and correlations with $O_3$ and formaldehyde (HCHO) that point to photochemically driven production.[87] Autumn observations in the rural North China Plain show that even under low-$NO_x$ conditions, rapid PAN formation can occur during haze events because HCHO photolysis and acetaldehyde oxidation significantly increase peroxyacetyl radical formation.[57]

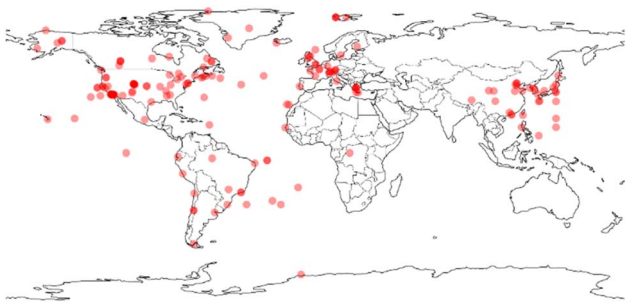

Fig. 7 World map showing the locations where PAN has been measured. Regions appear darker red the more extensively they have been studied.

Fig. 9 World map showing the locations where PAN has been measured in rural regions. Regions appear darker red the more extensively they have been studied.[35,41,43,55,57,81,85,92,93,97,98,100,102,113,115,118,133,160,165,180,197,207–229]

Fig. 10 World map showing the locations where PAN has been measured in polar regions. Regions appear darker red the more extensively they have been studied.[70,80,107,218,230–239]

Fig. 11 World map showing the locations where PAN has been measured in marine regions. Regions appear darker red the more extensively they have been studied.[81,103,105,108,111–114,128,135,153,184,230,240–244]

Fig. 12 World map showing the locations where PAN has been measured indoors. Regions appear darker red the more extensively they have been studied.[245–248]

### 6.3 Marine

Marine PAN levels are generally low because $NO_x$ concentrations are small and temperatures are cooler, promoting PAN stability but limiting production. Early measurements detected background PAN of 7–10 ppt in clean marine environments,[113] and modern campaigns confirm persistent low-ppt levels across the remote oceans.[113,218] While local PAN production is limited, marine regions often receive long-range PAN transport from continental outflow, especially during spring and periods of enhanced westerly flow. PAN can thus serve as a tracer of intercontinental pollution transport, with decomposition in the free troposphere supplying $NO_x$ that shapes photochemistry far from source regions.[208,216] Marine stratocumulus layers and cold oceanic boundary layers further reinforce PAN's role as a long-lived, temperature-controlled $NO_x$ reservoir.

Global trends show decreasing PAN in many regions, possibly driven by climate-related changes in temperature, radiation, and meteorology.[154] PAN is more abundant in the Northern Hemisphere due to greater anthropogenic and fire-related VOC emissions.[219] Early global measurements found background PAN in clean marine environments at 7–10 ppt,[113] and modern observations confirm PAN's presence throughout the free troposphere and upper troposphere and lower stratosphere (UTLS).[113,218] In some remote regions, PAN decomposition can explain all observed $NO_x$ in the free troposphere.[216]

### 6.4 Polar

Polar regions provide natural laboratories for studying PAN at extremely low temperatures, where its lifetime can reach months. In the Arctic and Antarctic free troposphere, PAN frequently constitutes a major fraction of total $NO_y$, in some cases approaching 50–90%.[33,34] The long lifetime allows efficient accumulation and transport, and high-latitude PAN abundances are strongly influenced by boreal wildfire emissions and long-range transport from midlatitudes. Siberian biomass burning contributes ~21% of PAN variability observed across western North America, with pronounced springtime enhancements.[209] At ground level, cold temperatures slow thermal decomposition significantly, and PAN can persist overnight or through multi-day stagnation events. Although observations are fragmentary compared to those at midlatitudes, available data consistently highlight the central role of PAN in polar $NO_y$ partitioning and long-range nitrogen redistribution.

### 6.5 Indoor

Although most PAN research has focused on outdoor and free-tropospheric environments, several studies show that PAN also occurs indoors at measurable levels. Indoor PAN arises from a combination of outdoor infiltration and indoor photochemical production, and its behavior has direct implications for sampling strategy, instrument placement, and interpretation of measured concentrations. Measurements in a near-zero-energy building (nZEB) in Sweden reported baseline indoor PAN levels of ~0.3 ppb under unoccupied conditions and up to ~1 ppb when the space was occupied.[245] These enhancements were attributed to reactions involving $O_3$, nitrogen dioxide, terpenes, and acetaldehyde, some of which were emitted from the spruce wood construction materials.[245] With adequate mechanical ventilation, PAN concentrations declined to levels below concern, underscoring the dominant role of ventilation efficiency.

Indoor PAN measurements in museums and conservation environments show concentrations up to ~0.7 ppb, primarily driven by outdoor infiltration, and highlight PAN's role in oxidative damage to sensitive materials.[246,251]

Natural ventilation strongly increases indoor PAN infiltration, with indoor/outdoor ratios often approaching unity under open-window conditions. Once buildings are sealed, indoor

PAN concentrations decrease rapidly due to thermal decomposition and limited internal sources.[247,252]

Indoor PAN chemistry nevertheless remains sparsely studied. A Monte Carlo analysis using the INDCM model showed that uncertainties in input parameters (*e.g.*, air exchange rate, radical production, and material sinks) can significantly influence predicted indoor PAN behavior, highlighting the need for improved indoor mechanistic treatment.[253] Recent work has also shown that cooking can generate measurable PAN indoors, providing one of the few demonstrated indoor sources.[254,255] These findings highlight that indoor PAN variability is dominated by ventilation, infiltration efficiency, and rapid thermal decomposition, with important implications for sampling strategy. Because indoor PAN lifetimes are short and infiltration-driven variability is high, minimizing residence times in sampling lines and controlling inlet temperatures are essential to prevent thermal decomposition losses during measurement.

### 6.6 Biomass burning

Increasing wildfire activity in many regions has renewed attention to PAN as a key mediator of long-range reactive nitrogen export from biomass-burning plumes. Biomass burning represents one of the most important episodic sources of PAN globally. Field campaigns in African savanna fires and boreal wildfire plumes consistently show large PAN enhancements associated with rapid photochemical processing of fire-emitted carbonyls and oxygenated VOCs.[31,32] Because PAN lifetimes increase strongly at low temperatures, lofted biomass-burning plumes often transport PAN efficiently over regional to hemispheric scales. Long-range transport from Siberian and trans-Pacific fire emissions has been shown to contribute substantially to PAN variability in downwind regions.[209] Observations further indicate that PAN production in biomass-burning plumes is tightly coupled to plume aging and secondary oxidation chemistry, reinforcing PAN's role as a key mediator of long-range reactive nitrogen redistribution.[31,85] These observations demonstrate that biomass-burning plumes represent one of the dominant pathways for PAN injection into the free troposphere, where subsequent thermal decomposition regulates regional ozone formation far from source regions.

PAN also contributes to $PM_{2.5}$ interactions: polluted environments show faster PAN production and higher mean values.[202] Biomass burning produces large spikes in PAN in Africa,[221] and PAN/PAA (peroxyacetic acid) ratios are useful indicators of plume age.[128] Overall, PAN chemistry is highly nonlinear, seasonally variable, and tightly coupled to VOC oxidation, $NO_x$ availability, transport, and atmospheric stability.

## 7 Past and future perspectives

### 7.1 Analysis

Taken together, historical observations, laboratory measurements, and multi-scale modeling studies show that PAN has moved from a "mysterious smog oxidant" to a central organizing species in tropospheric reactive nitrogen chemistry. Early work in Los Angeles and other polluted cities established PAN as a strong eye irritant, a phytotoxin, and a key product of hydrocarbon–$NO_x$ photochemistry, with peak mid-20th-century concentrations reaching tens of ppb in urban cores. Long-term monitoring now demonstrates that these extreme levels have declined substantially in response to coordinated $NO_x$ and VOC emission controls, even though modern megacities still experience short-lived PAN enhancements during stagnation events and wildfire intrusions.

Across environments, PAN behaves as both a sensitive, under-utilized diagnostic of photochemical processing and a dominant reservoir for $NO_x$, especially in cold, elevated, or remote air masses. Temperature-dependent lifetimes of minutes in the warm boundary layer *versus* months in the cold upper troposphere allow PAN to accumulate aloft and in export plumes, then decompose to release $NO_2$ downwind, sustaining $O_3$ formation far from the original emission regions. Aircraft, regional, and global models all highlight cases where PAN accounts for a large fraction of $NO_y$, particularly in the free troposphere, Arctic, and biomass-burning plumes. This reinforces the view that PAN is a controlling term in the long-range redistribution of reactive nitrogen rather than a minor by-product.

Observation-constrained box models and controlled smog-chamber experiments further show that PAN formation is strongly nonlinear with respect to its precursors. PAN isopleths consistently indicate regimes that are overwhelmingly VOC-limited, broadly similar in shape to $O_3$ isopleths but shifted toward higher VOC/$NO_x$ ratios. These studies quantify the dominant role of carbonyls and other oxygenated VOCs in PAN production, and they also reveal that PAN formation can simultaneously sequester $NO_x$, suppress $HO_x$ and $O_3$ production locally, and yet enhance $O_3$ formation downwind when PAN decomposes. Classic and modern chamber studies provide the experimental basis for these nonlinear sensitivities and continue to serve as critical benchmarks for evaluating chemical mechanisms used in regional and global models.

PAN sits at the intersection of gas- and particle-phase chemistry. Field campaigns in polluted and haze-prone environments show that PAN correlates with elevated $PM_{2.5}$, reflecting shared photochemical precursors and enhanced oxidative processing. Laboratory work indicates that PAN undergoes small but non-negligible heterogeneous uptake on real-world aerosols, generating particulate nitrate and oxidized organic fragments, while related peroxyacyl nitrates such as MPAN participate in high-$NO_x$ SOA formation pathways. PAN therefore acts more as a facilitator and indicator of secondary aerosol formation than as a direct nucleating vapor.

Indoor and cultural-heritage studies add a complementary perspective, demonstrating that PAN infiltrates indoors, contributes to material damage in sensitive environments, and responds to building operation and indoor VOC sources.

Overall, the literature portrays PAN as an integrating species that links local photochemical smog, long-range $NO_x$ transport, aerosol chemistry, and climate-driven changes in temperature and circulation. The same properties that once made PAN a nuisance in early smog studies now make it one of the most

informative tracers of modern atmospheric oxidation and reactive nitrogen budgets.

### 7.2 Gaps in PAN research

Despite this mature picture, several important gaps limit the use of PAN as a fully quantitative constraint on atmospheric chemistry. First, the global PAN observing system remains sparse. Long, high-quality time series are concentrated in a few North American, European, and East Asian regions, while measurements in the tropics, Southern Hemisphere, high latitudes, and over the oceans are fragmented or absent. Vertical coverage is limited: aircraft campaigns are episodic, and there are few routine free-tropospheric or lower-stratospheric PAN observations, even though these layers are where PAN lifetimes are longest and its role in $NO_y$ export is greatest.

Second, PAN's multiphase and heterogeneous behavior is still poorly constrained. Existing laboratory studies point to nonzero uptake on real-world $PM_{2.5}$ and potential reactions on carbonaceous and PAH-rich aerosol, but the magnitude, product distributions, and environmental dependence of these processes remain uncertain. The role of aerosol-mediated radical chemistry in sustaining PAN production during severe haze episodes is also not fully quantified. Similarly, indoor PAN chemistry has only been explored in a small number of buildings and museums, leaving open questions about how building materials, ventilation strategies, and indoor VOC mixtures shape PAN lifetimes and impacts on human health and cultural heritage.

Third, models still struggle to reproduce observed PAN abundances and variability. Persistent underestimates in box, regional, and global simulations have been attributed to insufficient treatment of regional and vertical transport, incomplete VOC oxidation schemes (particularly for multifunctional carbonyls and biomass-burning tracers), and oversimplified deposition and heterogeneous loss parameterizations. PAN isopleths and PAN–$O_3$ relationships are not yet routinely used as evaluation tools in chemistry–climate and air-quality models, even though they provide a compact way to test whether mechanisms capture the correct nonlinear sensitivity to VOC and $NO_x$ emissions.

Fourth, climate-driven changes in temperature, circulation, wildfire activity, and VOC emission patterns are expected to reshape PAN formation and transport, yet there are relatively few coordinated studies linking long-term PAN trends to these drivers. Existing analyses suggest that global PAN concentrations may have declined alongside $NO_x$ emissions in some regions while also responding to shifts in meteorology and biomass burning, but this emerging picture is incomplete. Addressing these gaps will require integrated efforts that couple targeted laboratory work, expanded measurement networks (including indoors), and model experiments that explicitly treat PAN as a diagnostic of both chemistry and climate forcing. Modeling studies need to be improved to better study PAN–aerosol interactions, fuel-change impacts, and PAN urban-boundary layer chemistry.

Beyond scientific gaps, there are also public-communication and policy gaps. Current air-quality indices (*e.g.*, the U.S. AQI) do not explicitly include PAN, despite its role as a potent irritant and an important $NO_x$ reservoir. Episodes in historically polluted regions such as Los Angeles and modern megacities such as Beijing demonstrate that PAN can reach levels of health concern even when AQI categories are driven primarily by $O_3$ and $PM_{2.5}$. This mismatch suggests that future AQI frameworks or supplemental indices may need to treat PAN more explicitly, particularly during strong photochemical smog events.

A final area of limited understanding involves meteorological regimes. Despite extensive work on PAN in urban, free-tropospheric, and biomass-burning environments, PAN behavior under persistent cold-pool inversions remains poorly characterized. Stable boundary layers common in basins and mountain valleys suppress vertical mixing, sharply reduce thermal decomposition rates, and can allow PAN to accumulate even when precursor VOCs and $NO_x$ are low. Preliminary field campaigns in western North America suggest that nighttime PAN formation *via* $NO_3$ chemistry and potential heterogeneous production on ice-coated surfaces may be enhanced during multi-day inversion events. Because these conditions are frequent in wintertime basins and can strongly influence $O_3$ buildup during inversion breakup, dedicated studies integrating meteorology, nighttime chemistry, and heterogeneous processes are needed to understand PAN budgets in these regimes.

## 8 Conclusions

Despite more than five decades of study, PAN remains treated inconsistently across atmospheric chemistry subdisciplines, alternately framed as a passive $NO_y$ reservoir, a diagnostic of photochemical aging, or a secondary pollutant of limited regulatory relevance. This review demonstrates that such compartmentalized interpretations obscure PAN's central role in coupling hydrocarbon oxidation, nitrogen transport, and thermal stability across spatial and temporal scales. We show that uncertainties in PAN measurement techniques, thermal decomposition kinetics, and precursor attribution propagate directly into errors in inferred $NO_x$ lifetimes, regional ozone production efficiency, and model–observation closure. As a result, PAN is not merely under-measured, but systematically misinterpreted. Reconciling these inconsistencies is essential for accurately diagnosing oxidative capacity in both polluted and remote environments and for improving the treatment of reactive nitrogen in chemical transport models under changing climate conditions.

Peroxyacetyl nitrate (PAN) is now recognized as a cornerstone species in tropospheric chemistry. Formed entirely *in situ* from VOC oxidation in the presence of $NO_2$, PAN exhibits a strongly temperature-dependent lifetime and serves as a major reservoir and long-range transport vector for $NO_x$ from the boundary layer to the free troposphere and lower stratosphere. Historical and modern observations demonstrate that PAN links local photochemical smog to downwind $O_3$ formation, vegetation injury, indoor air quality, and background oxidant levels far from emission sources.

This review has synthesized the current understanding of PAN's formation pathways, loss processes, measurement

techniques, and roles in smog chemistry, $NO_y$ partitioning, aerosol formation, and regional background $O_3$. Laboratory and theoretical work have established robust kinetic parameters, absorption cross-sections, and quantum yields, enabling quantitative PAN detection from the UV to the IR. Field observations across urban, rural, remote, biomass-burning, and indoor environments show that PAN is both a sensitive indicator of photochemical processing and a powerful tracer of long-range pollution transport. Modeling studies, from box models to global chemistry–climate simulations, highlight PAN's nonlinear response to VOC and $NO_x$ controls and its usefulness as an under-utilized diagnostic of chemical mechanisms, precursor emissions, and transport regimes.

At the same time, important uncertainties remain. Sparse spatial and vertical observational coverage, incomplete representation of heterogeneous and indoor processes, and persistent model–measurement gaps still limit the use of PAN as a fully quantitative constraint on oxidant chemistry and $NO_y$ budgets. PAN behavior under cold-pool inversions and other stable boundary-layer regimes is poorly characterized despite its potential importance for wintertime basins and downwind $O_3$ buildup. Climate-driven shifts in temperature, circulation, and wildfire activity are likely to further reshape PAN distributions and lifetimes. Additionally, PAN is not explicitly included in current air-quality indices, even though it is a potent irritant and can reach levels of health concern during strong photochemical smog events.

Addressing these gaps will require targeted laboratory studies, expanded measurement networks (including routine free-tropospheric and indoor observations), and model experiments that treat PAN explicitly as both a chemical species and a diagnostic of VOC–$NO_x$–oxidant interactions. With improved mechanistic and observational constraints, PAN can serve as an even more powerful integrative tool for evaluating atmospheric chemistry, interpreting long-range transport, and guiding air-quality and climate-chemistry assessment in a rapidly changing world. Future progress in PAN research will depend on integrating emerging multiphase chemistry, climate-driven emission changes, and improved representation in Earth-system models.

## Author contributions

C. E. F.: conceptualization, investigation, data curation, analysis, visualization, and writing – original draft. J. C. H.: supervision, funding acquisition, and writing – review and editing.

## Conflicts of interest

The authors declare that there are no conflicts of interest.

## Data availability

This review did not generate new data. All data discussed are available in the cited literature and in the supplementary information (SI). Supplementary information: tables used to create Fig. 7–12. See DOI: https://doi.org/10.1039/d6ea00017g.

## Acknowledgements

Brigham Young University, College of Physical and Mathematical Studies, paid the graduate student salary.

## References

1 T. L. Mazely, R. R. Friedl and S. P. Sander, Production of $NO_2$ from photolysis of peroxyacetyl nitrate, *J. Phys. Chem.*, 1995, **99**, 8162–8169.
2 E. R. Stephens, P. L. Hanst, R. C. Doerr and W. E. Scott, Reactions of nitrogen dioxide and organic compounds in air, *Ind. Eng. Chem.*, 1956, **48**, 1498–1504.
3 E. R. Stephens, W. E. Scott, P. L. Hanst and R. C. Doerr, Recent Developments in the Study of the Organic Chemistry of the Atmosphere, *J. Air Pollut. Control Assoc.*, 1956, **6**, 159–165.
4 E. R. Stephens, Smog studies of the 1950s, *Trans., Am. Geophys. Union*, 1987, **68**, 89–93.
5 E. C. Tuazon, R. A. Graham, A. M. Winer, R. R. Easton, J. N. Pitts and P. L. Hanst, Kilometer pathlength fourier-transform infrared system for study of trace pollutants in ambient and synthetic atmospheres, *Atmos. Environ.*, 1978, **12**, 865–875.
6 P. L. Hanst, N. W. Wong and J. Bragin, A long-path infrared study of Los-Angeles SMOG, *Atmos. Environ.*, 1982, **16**, 969–981.
7 E. F. Darley, E. R. Stephens and K. A. Kettner, Analysis of peroxyacyl nitrates by gas chromatography with electron capture detection, *Anal. Chem.*, 1963, **35**, 589.
8 H. B. Singh, L. J. Salas and W. Viezee, Global distribution of peroxyacetyl nitrate, *Nature*, 1986, **321**, 588–591.
9 J. E. Lovelock and S. A. Penkett, PAN over the Atlantic and the smell of clean linen, *Nature*, 1974, **249**, 434.
10 J. F. Kasting and H. B. Singh, Nonmethane hydrocarbons in the troposphere - impact on the odd hydrogen and odd nitrogen chemistry, *J. Geophys. Res.:Atmos.*, 1986, **91**, 3239–3256.
11 A. C. Aikin, J. R. Herman, E. J. R. Maier and C. J. McQuillan, Influence of peroxyacetyl nitrate (PAN) on odd nitrogen in the troposphere and lower stratosphere, *Planet. Space Sci.*, 1983, **31**, 1075–1082.
12 M. Rolletter, E. Assaf, M. Assali, H. Fuchs and C. Fittschen, The absorption spectrum and absolute absorption cross sections of acetylperoxy radicals, $CH_3C(O)O_2$ in the near IR, *J. Quant. Spectrosc. Radiat. Transfer*, 2020, **245**, 106877.
13 E. V. Fischer, D. J. Jacob, R. M. Yantosca, M. P. Sulprizio, D. B. Millet, J. Mao, F. Paulot, H. B. Singh, A. Roiger, L. Ries, R. W. Talbot, K. Dzepina and S. Pandey Deolal, Atmospheric peroxyacetyl nitrate (PAN): a global budget and source attribution, *Atmos. Chem. Phys.*, 2014, **14**, 2679–2698.
14 G. Allen, J. J. Remedios, D. A. Newnham, K. M. Smith and P. S. Monks, Improved mid-infrared cross-sections for peroxyacetyl nitrate (PAN) vapour, *Atmos. Chem. Phys.*, 2005, **5**, 47–56.
15 W. J. Moxim, H. Levy and P. S. Kasibhatla, Simulated global tropospheric PAN: Its transport and impact on NOx, *J. Geophys. Res.:Atmos.*, 1996, **101**, 12621–12638.

16 I. Barnes, K. H. Becker and T. Zhu, Near UV absorption spectra and photolysis products of difunctional organic nitrates: Possible importance as NOxreservoirs, *J. Atmos. Chem.*, 1993, **17**, 353–373.
17 H. B. Singh, L. J. Salas, B. A. Ridley, J. D. Shetter, N. M. Donahue, F. C. Fehsenfeld, D. W. Fahey, D. D. Parrish, E. J. Williams, S. C. Liu, G. Hubler and P. C. Murphy, Relationship between peroxyacetyl nitrate and nitrogen-oxides in the clean troposphere, *Nature*, 1985, **318**, 347–349.
18 P. B. Shepson, D. R. Hastie, K. W. So and H. I. Schiff, Relationships between PAN, PPN and $O_3$ at urban and rural sites in Ontario, *Atmos. Environ., Part A*, 1992, **26**, 1259–1270.
19 R. G. Derwent and M. E. Jenkin, Hydrocarbons and the long-range transport of ozone and pan across Europe, *Atmos. Environ., Part A*, 1991, **25**, 1661–1678.
20 P. S. Kasibhatla, H. Levy and W. J. Moxim, Global $NO_X$, $HNO_3$, PAN, and $NO_Y$ distributions from fossil-fuel combustion emissions - a model study, *J. Geophys. Res.:Atmos.*, 1993, **98**, 7165–7180.
21 R. E. Honrath and D. A. Jaffe, The seasonal cycle of nitrogen-oxides in the arctic troposphere at Barrow, Alaska, *J. Geophys. Res.:Atmos.*, 1992, **97**, 20615–20630.
22 H. B. Singh, D. Ohara, D. Herlth, J. D. Bradshaw, S. T. Sandholm, G. L. Gregory, G. W. Sachse, D. R. Blake, P. J. Crutzen and M. A. Kanakidou, Atmospheric measurements of peroxyacetyl nitrate and other organic nitrates at high-latitudes - possible sources and sinks, *J. Geophys. Res.:Atmos.*, 1992, **97**, 16511–16522.
23 D. D. Parrish, C. J. Hahn, E. J. Williams, R. B. Norton, F. C. Fehsenfeld, H. B. Singh, J. D. Shetter, B. W. Gandrud and B. A. Ridley, Indications of photochemical histories of pacific air masses from measurements of atmospheric trace species at Point Arena, California, *J. Geophys. Res.:Atmos.*, 1992, **97**, 15883–15901.
24 J. J. Orlando, G. S. Tyndall and J. G. Calvert, Thermal-decomposition pathways for peroxyacetyl nitrate (PAN) - implications for atmospheric methyl nitrate levels, *Atmos. Environ., Part A*, 1992, **26**, 3111–3118.
25 J. M. Roberts and S. B. Bertman, The thermal-decomposition of peroxyacetic nitric anhydride (PAN) and peroxymethacrylic nitric anhydride (MPAN), *Int. J. Chem. Kinet.*, 1992, **24**, 297–307.
26 D. Grosjean, E. Grosjean and E. L. Williams, Formation and thermal-decomposition of butyl-substituted peroxyacyl nitrates - n-C4H9C(O)OONO2 and i-C4H9C(O)OONO2, *Environ. Sci. Technol.*, 1994, **28**, 1099–1105.
27 R. K. Talukdar, J. B. Burkholder, A. M. Schmoltner, J. M. Roberts, R. R. Wilson and A. R. Ravishankara, Investigation of the loss processes for peroxyacetyl nitrate in the atmosphere - UV photolysis and reaction with OH, *J. Geophys. Res.:Atmos.*, 1995, **100**, 14163–14173.
28 T. J. Wallington, R. Atkinson and A. M. Winer, Rate constants for the gas-phase reaction of OH radicals with peroxyacetyl nitrate (PAN) at 273-K and 297-K, *Geophys. Res. Lett.*, 1984, **11**, 861–864.
29 N. Tsalkani, A. Mellouki, G. Poulet, G. Toupance and G. Lebras, Rate-constant measurement for the reactions of OH and Cl with peroxyacetyl nitrate at 298-K, *J. Atmos. Chem.*, 1988, **7**, 409–419.
30 T. J. Wallington, J. M. Andino, J. C. Ball and S. M. Japar, Fourier-transform infrared studies of the reaction of cl atoms with PAN, PPN, $CH_3OOH$, HCOOH, $CH_3COCH_3$ AND $CH_3COC_2H_5$ AT 295+-2-K, *J. Atmos. Chem.*, 1990, **10**, 301–313.
31 M. W. Holdren, C. W. Spicer and J. M. Hales, Peroxyacetyl nitrate solubility and decomposition rate in acidic water, *Atmos. Environ.*, 1984, **18**, 1171–1173.
32 S. Langer, I. Wangberg and E. Ljungstrom, Heterogeneous transformation of peroxyacetylnitrate, *Atmos. Environ., Part A*, 1992, **26**, 3089–3098.
33 J. W. Bottenheim, A. G. Gallant and K. A. Brice, Measurements of NOY species and O3 at 82° N latitude, *Geophys. Res. Lett.*, 1986, **13**, 113–116.
34 B. P. Finlayson-Pitts and J. Pitts, *Chemistry of the Upper and Lower Atmosphere*, Academic Press, 2000.
35 C. Keim, G. Y. Liu, C. E. Blom, H. Fischer, T. Gulde, M. Höpfner, C. Piesch, F. Ravegnani, A. Roiger, H. Schlager and N. Sitnikov, Vertical profile of peroxyacetyl nitrate (PAN) from MIPAS-STR measurements over Brazil in February 2005 and its contribution to tropical UT NOy partitioning, *Atmos. Chem. Phys.*, 2008, **8**, 4891–4902.
36 G. Daocheng, M. Liao, G. Wu, H. Wang, Q. Li, Y. Chen, S. Deng, Y. Zheng, J. Ou and B. Wang, Characteristics of peroxyacetyl nitrate (PAN) in the high-elevation background atmosphere of South-Central China: Implications for regional photochemical pollution, *Atmos. Environ.*, 2021, **254**, 118424.
37 A. P. Altshuller, Measurements of the products of atmospheric photochemical reactions in laboratory studies and in ambient air-relationships between ozone and other products, *Atmos. Environ.*, 1983, (17), 2383–2427.
38 C. M. Li, Z. Bi, H. C. Wang and K. D. Lu, Field Measurement of Alkyl Nitrates in the Atmosphere, *Acta Chim. Sin.*, 2024, **82**, 323–335.
39 Z. Y. Lin, L. L. Xu, C. Yang, G. J. Chen, X. T. Ji, L. J. Li, K. R. Zhang, Y. W. Hong, M. R. Li, X. L. Fan, B. Y. Hu, F. W. Zhang and J. S. Chen, Trends of peroxyacetyl nitrate and its impact on ozone over 2018-2022 in urban atmosphere, *npj Clim. Atmos. Sci.*, 2024, **7**, 129.
40 X. Q. Qiao, M. Sun, Y. F. Wang, D. Zhang, R. Q. Zhang, B. Zhao and J. B. Zhang, Strong relations of peroxyacetyl nitrate (PAN) formation to alkene and nitrous acid during various episodes, *Environ. Pollut.*, 2023, **326**, 121465.
41 B. Wang, M. Shao, J. M. Roberts, G. Yang, F. Yang, M. Hu, L. Zeng, Y. Zhang and J. Zhang, Ground-based on-line measurements of peroxyacetyl nitrate (PAN) and peroxypropionyl nitrate (PPN) in the Pearl River Delta, China, *Int. J. Environ. Anal. Chem.*, 2010, **90**, 548–559.
42 M. A. Rubio, P. Oyola, E. Gramsch, E. Lissi, J. Pizarro and G. Villena, Ozone and peroxyacetylnitrate in downtown Santiago, Chile, *Atmos. Environ.*, 2004, **38**, 4931–4939.

43 B. Rappenglück, D. Melas and P. Fabian, Evidence of the impact of urban plumes on remote sites in the Eastern Mediterranean, *Atmos. Environ.*, 2003, **37**, 1853–1864.
44 A. P. Altshuller, Pans in the atmosphere, *J. Air Waste Manage. Assoc.*, 1993, **43**, 1221–1230.
45 M. Yukihiro, T. Hiramatsu, F. Bouteau, T. Kadono and T. Kawano, Peroxyacetyl nitrate-induced oxidative and calcium signaling events leading to cell death in ozone-sensitive tobacco cell-line, *Plant Signaling Behav.*, 2012, **7**, 113–120.
46 A. J. Haagen-Smit, E. F. Darley, M. Zaitlin, H. Hull and W. Noble, Investigation on Injury to Plants from Air Pollution in the Los Angeles Area, *Plant Physiol.*, 1952, **27**, 18–34.
47 T. A. Teklemariam and J. P. Sparks, Gaseous fluxes of peroxyacetyl nitrate (PAN) into plant leaves, *Plant, Cell Environ.*, 2004, **27**, 1149–1158.
48 P. J. Temple and O. C. Taylor, Combined effects of peroxyacetyl nitrate and ozone on growth of 4 tomato cultivars, *J. Environ. Qual.*, 1985, **14**, 420–424.
49 J. T. Metzler and E. J. Pell, The impact of peroxyacetyl nitrate on conductance of bean-leaves and on associated cellular and foliar symptom expression, *Phytopathology*, 1980, **70**, 934–938.
50 J. P. Sparks, J. M. Roberts and R. K. Monson, The uptake of gaseous organic nitrogen by leaves: A significant global nitrogen transfer process, *Geophys. Res. Lett.*, 2003, **30**, 2189.
51 A. Vyskocil, C. Viau and S. Lamy, Peroxyacetyl nitrate: review of toxicity, *Hum. Exp. Toxicol.*, 1998, **17**, 212–220.
52 T. E. Kleindienst, P. B. Shepson, D. F. Smith, E. E. Hudgens, C. M. Nero, L. T. Cupitt, J. J. Bufalini and L. D. Claxton, Comparison of mutagenic activities of several peroxyacyl nitrates, *Environ. Mol. Mutagen.*, 1990, **16**, 70–80.
53 D. M. DeMarini, M. L. Shelton, M. J. Kohan, E. E. Hudgens, T. E. Kleindienst, L. M. Ball, D. Walsh, J. G. de Boer, L. Lewis-Bevan, J. R. Rabinowitz, L. D. Claxton and J. Lewtas, Mutagenicity in lung of Big Blue® mice and induction of tandem-base substitutions in Salmonella by the air pollutant peroxyacetyl nitrate (PAN): predicted formation of intrastrand cross-links, *Mutat. Res., Fundam. Mol. Mech. Mutagen.*, 2000, **457**, 41–55.
54 J. S. Gaffney and N. A. Marley, The Impacts of Peroxyacetyl Nitrate in the Atmosphere of Megacities and Large Urban Areas: A Historical Perspective, *ACS Earth Space Chem.*, 2021, **5**, 1829–1841.
55 J. M. Roberts, R. L. Tanner, L. Newman, V. C. Bowersox, J. W. Bottenheim, K. G. Anlauf, K. A. Brice, D. D. Parrish, F. C. Fehsenfeld, M. P. Buhr, J. F. Meagher and E. M. Bailey, Relationships between pan and ozone at sites in eastern North-America, *J. Geophys. Res.:Atmos.*, 1995, **100**, 22821–22830.
56 J. H. P. Seinfeld and S. P. Pandis, *Atmospheric Chemistry and Physics: from Air Pollution to Climate Change*, Wiley-Interscience, 1998.
57 Y. L. Qiu, Z. Q. Ma, K. Li, M. Y. Huang, J. J. Sheng, P. Tian, J. Zhu, W. W. Pu, Y. X. Tang, T. T. Han, H. G. Zhou and H. Liao, Measurement report: Fast photochemical production of peroxyacetyl nitrate (PAN) over the rural North China Plain during haze events in autumn, *Atmos. Chem. Phys.*, 2021, **21**, 17995–18010.
58 H. B. Singh, in *Encyclopedia of Atmospheric Sciences*, ed. G. R. North, J. Pyle and F. Zhang, Academic Press, Oxford, 2nd edn, 2015, pp. 251–254, DOI: 10.1016/B978-0-12-382225-3.00433-3.
59 H. Zhang, S. Tong, W. Zhang, Y. Xu, M. Zhai, Y. Guo, X. Li, L. Wang, G. Tang, Z. Liu, B. Hu, C. Liu, P. Liu, X. Sun, Y. Mu and M. Ge, A comprehensive observation on the pollution characteristics of peroxyacetyl nitrate (PAN) in Beijing, China, *Sci. Total Environ.*, 2023, **905**, 166852.
60 J. G. Murphy, A. Day, P. A. Cleary, P. J. Wooldridge and R. C. Cohen, Observations of the diurnal and seasonal trends in nitrogen oxides in the western Sierra Nevada, *Atmos. Chem. Phys.*, 2006, **6**, 5321–5338.
61 P. Suppan, P. Fabian, L. Vyras and S. E. Gryning, The behaviour of ozone and peroxyacetyl nitrate concentrations for different wind regimes during the MEDCAPHOT-TRACE campaign in the greater area of Athens, Greece, *Atmos. Environ.*, 1998, **32**, 2089–2102.
62 S. Glavas and U. Schurath, Peroxyacetyl nitrate forming potential of five prototype hydrocarbons, *Environ. Sci. Technol.*, 1985, **19**, 950–955.
63 J. Kames, S. Schweighoefer and U. Schurath, Henrys law constant and hydrolysis of peroxyacetyl nitrate (PAN), *J. Atmos. Chem.*, 1991, **12**, 169–180.
64 C. A. Cantrell, J. A. Davidson, K. L. Busarow and J. G. Calvert, The $CH_3CHO$-$NO_3$ reaction and possible nighttime pan generation, *J. Geophys. Res.:Atmos.*, 1986, **91**, 5347–5353.
65 S. Sillman, J. A. Logan and S. C. Wofsy, The sensitivity of ozone to nitrogen-oxides and hydrocarbons in regional ozone episodes, *J. Geophys. Res.:Atmos.*, 1990, **95**, 1837–1851.
66 B. A. Flowers, M. E. Angerhofer, W. R. Simpson, T. Nakayama and Y. Matsumi, Nitrate Radical Quantum Yield from Peroxyacetyl Nitrate Photolysis, *J. Phys. Chem. A*, 2005, **109**, 2552–2558.
67 A. C. Hill, Vegetation - sink for atmospheric pollutants, *J. Air Pollut. Control Assoc.*, 1971, **21**, 341.
68 J. A. Garland and S. A. Penkett, Absorption of peroxy acetyl nitrate and ozone by natural surfaces, *Atmos. Environ.*, 1976, (10), 1127–1131.
69 T. E. Kleindienst, Recent developments in the chemistry and biology of peroxyacetyl nitrate, *Res. Chem. Intermed.*, 1994, **20**, 335–384.
70 J. M. Roberts, D. D. Parrish, R. B. Norton, S. B. Bertman, J. S. Holloway, M. Trainer, F. C. Fehsenfeld, M. A. Carroll, G. M. Albercook, T. Wang and G. Forbes, Episodic removal of NOy species from the marine boundary layer over the North Atlantic, *J. Geophys. Res.:Atmos.*, 1996, **101**, 28947–28960.
71 R. E. Honrath, A. J. Hamlin and J. T. Merrill, Transport of ozone precursors from the Arctic troposphere to the

North Atlantic region, *J. Geophys. Res.:Atmos.*, 1996, **101**, 29335–29351.

72 J. Kames and U. Schurath, Alkyl nitrates and bifunctional nitrates of atmospheric interest - henry law constants and their temperature dependencies, *J. Atmos. Chem.*, 1992, **15**, 79–95.

73 R. Atkinson, Gas-phase tropospheric chemistry of volatile organic compounds. 1. Alkanes and alkenes, *J. Phys. Chem. Ref. Data*, 1997, **26**, 215–290.

74 L. Jet Propulsion, *Chemical Kinetics and Photochemical Data for Use in Atmospheric Studies, Evaluation No. 19*, JPL Publication, 19-5, Pasadena, California, USA, 2019.

75 J. B. Burkholder, S. P. Sander, J. P. D. Abbatt, J. R. Barker, C. Cappa, J. D. Crounse, T. S. Dibble, R. E. Huie, C. E. Kolb, M. J. Kurylo, V. L. Orkin, C. J. Percival, D. M. Wilmouth, P. H. Wine, *Chemical Kinetics and Photochemical Data for Use in Atmospheric Studies, Evaluation No. 19, JPL Publication 19-5*, 2019.

76 NCAR, Tropospheric Ultraviolet and Visible (TUV) Radiation Model, https://www2.acom.ucar.edu/modeling/tropospheric-ultraviolet-and-visible-tuv-radiation-model, accessed 10 February 2023.

77 T. L. Mazely, R. R. Friedl and S. P. Sander, Quantum yield of NO3 from peroxyacetyl nitrate photolysis, *J. Phys. Chem. A*, 1997, **101**, 7090–7097.

78 M. H. Harwood, J. M. Roberts, G. J. Frost, A. R. Ravishankara and J. B. Burkholder, Photochemical studies of $CH_3C(O)OONO_2$ (PAN) and $CH_3CH_2C(O)OONO_2$ (PPN):: $NO_3$ quantum yields, *J. Phys. Chem. A*, 2003, **107**, 1148–1154.

79 B. A. Flowers, J. F. Stanton and W. R. Simpson, Wavelength Dependence of Nitrate Radical Quantum Yield from Peroxyacetyl Nitrate Photolysis: Experimental and Theoretical Studies, *J. Phys. Chem. A*, 2007, **111**, 11602–11607.

80 G. J. Phillips, N. Pouvesle, J. Thieser, G. Schuster, R. Axinte, H. Fischer, J. Williams, J. Lelieveld and J. N. Crowley, Peroxyacetyl nitrate (PAN) and peroxyacetic acid (PAA) measurements by iodide chemical ionisation mass spectrometry: first analysis of results in the boreal forest and implications for the measurement of PAN fluxes, *Atmos. Chem. Phys.*, 2013, **13**, 1129–1139.

81 B. A. Ridley, J. D. Shetter, B. W. Gandrud, L. J. Salas, H. B. Singh, M. A. Carroll, G. Hubler, D. L. Albritton, D. R. Hastie, H. I. Schiff, G. I. Mackay, D. R. Karechi, D. D. Davis, J. D. Bradshaw, M. O. Rodgers, S. T. Sandholm, A. L. Torres, E. P. Condon, G. L. Gregory and S. M. Beck, Ratios of peroxyacetyl nitrate to active nitrogen observed during aircraft flights over the eastern Pacific Oceans and continental United-States, *J. Geophys. Res.:Atmos.*, 1990, **95**, 10179–10192.

82 F. Kirchner, A. Mayer-Figge, F. Zabel and K. H. Becker, Thermal stability of peroxynitrates, *Int. J. Chem. Kinet.*, 1999, **31**, 127–144.

83 J. B. Zhang, Z. Xu, G. Yang and B. Wang, Peroxyacetyl nitrate (PAN) and peroxypropionyl nitrate (PPN) in urban and suburban atmospheres of Beijing, China, *Atmos. Chem. Phys. Discuss.*, 2011, **2011**, 8173–8206.

84 E. C. Tuazon, R. A. Graham, A. M. Winer, R. R. Easton, J. N. Pitts and P. L. Hanst, A kilometer pathlength fourier-transform infrared system for the study of trace pollutants in ambient and synthetic atmospheres, *Atmos. Environ.*, 1978, (12), 865–875.

85 L. Zeng, G.-J. Fan, X. Lyu, H. Guo, J.-L. Wang and D. Yao, Atmospheric fate of peroxyacetyl nitrate in suburban Hong Kong and its impact on local ozone pollution, *Environ. Pollut.*, 2019, **252**, 1910–1919.

86 S. X. Zhai, D. J. Jacob, B. Franco, L. Clarisse, P. Coheur, V. R. Shah, K. H. Bates, H. P. Lin, R. J. Dang, M. P. Sulprizio, L. G. Huey, F. L. Moore, D. A. Jaffe and H. Liao, Transpacific Transport of Asian Peroxyacetyl Nitrate (PAN) Observed from Satellite: Implications for Ozone, *Environ. Sci. Technol.*, 2024, **58**, 9760–9769.

87 T. Liu, G. Chen, J. Chen, L. Xu, M. Li, Y. Hong, Y. Chen, X. Ji, C. Yang, Y. Chen, W. Huang, Q. Huang and H. Wang, Seasonal characteristics of atmospheric peroxyacetyl nitrate (PAN) in a coastal city of Southeast China: Explanatory factors and photochemical effects, *Atmos. Chem. Phys.*, 2022, **22**, 4339–4353.

88 E. R. Stephens, F. R. Burleson and K. M. Holtzclaw, A Damaging Explosion of Peroxyacetyl Nitrate, *J. Air Pollut. Control Assoc.*, 1969, **19**, 261–264.

89 T. Nielsen, A. M. Hansen and E. L. Thomsen, A convenient method for preparation of pure standards of peroxyacetyl nitrate for atmospheric analyses, *Atmos. Environ.*, 1982, **16**, 2447–2450.

90 J. S. Gaffney, R. Fajer and G. I. Senum, An improved procedure for high purity gaseous peroxyacyl nitrate production: Use of heavy lipid solvents, *Atmos. Environ.*, 1984, (18), 215–218.

91 A. Volz-Thomas, I. Xueref and R. Schmitt, An automatic gas chromatograph and calibration system for ambient measurements of PAN and PPN, *Environ. Sci. Pollut. Res.*, 2002, 72–76.

92 L. Zhang, D. A. Jaffe, X. Gao and C. D. McClure, A quantification method for peroxyacetyl nitrate (PAN) using gas chromatography (GC) with a non-radioactive pulsed discharge detector (PDD), *Atmos. Environ.*, 2018, **179**, 23–30.

93 E. V. Fischer, D. A. Jaffe, D. R. Reidmiller and L. Jaeglé, Meteorological controls on observed peroxyacetyl nitrate at Mount Bachelor during the spring of 2008, *J. Geophys. Res.:Atmos.*, 2010, **115**, D03302.

94 F. M. Flocke, A. J. Weinheimer, A. L. Swanson, J. M. Roberts, R. Schmitt and S. Shertz, On the Measurement of PANs by Gas Chromatography and Electron Capture Detection, *J. Atmos. Chem.*, 2005, **52**, 19–43.

95 P. Warneck and T. Zerbach, Synthesis of peroxyacetyl nitrate in air by acetone photolysis, *Environ. Sci. Technol.*, 1992, **26**, 74–79.

96 A. Furgeson, L. H. Mielke, D. Paul and H. D. Osthoff, A photochemical source of peroxypropionic and

peroxyisobutanoic nitric anhydride, *Atmos. Environ.*, 2011, **45**, 5025–5032.

97 Y. L. Qiu, Z. Q. Ma, K. Li, W. L. Lin, Y. X. Tang, F. Dong and H. Liao, Markedly Enhanced Levels of Peroxyacetyl Nitrate (PAN) During COVID-19 in Beijing, *Geophys. Res. Lett.*, 2020, **47**, e2020GL089623.

98 Y. Qiu, Z. Ma, W. Lin, W. Quan, W. Pu, Y. Li, L. Zhou and Q. Shi, A study of peroxyacetyl nitrate at a rural site in Beijing based on continuous observations from 2015 to 2019 and the WRF-Chem model, *Front. Environ. Sci. Eng.*, 2020, **14**, 71.

99 B. Rappenglück, K. Kourtidis and P. Fabian, Measurements of ozone and peroxyacetyl nitrate (pan) in Munich, *Atmos. Environ., Part B*, 1993, **27**, 293–305.

100 C. S. Malley, J. N. Cape, M. R. Jones, S. R. Leeson, M. Coyle, C. F. Braban, M. R. Heal and M. M. Twigg, Regional and hemispheric influences on measured spring peroxyacetyl nitrate (PAN) mixing ratios at the Auchencorth UK EMEP supersite, *Atmos. Res.*, 2016, **174–175**, 135–141.

101 J.-B. Lee, J.-S. Yoon, K. Jung, S.-W. Eom, Y.-Z. Chae, S.-J. Cho, S.-D. Kim, J. R. Sohn and K.-H. Kim, Peroxyacetyl nitrate (PAN) in the urban atmosphere, *Chemosphere*, 2013, **93**, 1796–1803.

102 S. Toma, S. Bertman, C. Groff, F. Xiong, P. B. Shepson, P. Romer, K. Duffey, P. Wooldridge, R. Cohen, K. Baumann, E. Edgerton, A. R. Koss, J. de Gouw, A. Goldstein, W. Hu and J. L. Jimenez, Importance of biogenic volatile organic compounds to acyl peroxy nitrates (APN) production in the southeastern US during SOAS 2013, *Atmos. Chem. Phys.*, 2019, **19**, 1867–1880.

103 J. W. Bottenheim and A. J. Gallant, The occurrence of peroxyacetyl nitrate over the Atlantic Ocean east of North America during WATOX-86, *Global Biogeochem. Cycles*, 1987, **1**, 369–380.

104 J. S. Gaffney, R. M. Bornick, Y. H. Chen and N. A. Marley, Capillary gas chromatographic analysis of nitrogen dioxide and PANs with luminol chemiluminescent detection, *Atmos. Environ.*, 1998, **32**, 1445–1454.

105 J. M. Roberts, M. Marchewka, S. B. Bertman, R. Sommariva, C. Warneke, J. de Gouw, W. Kuster, P. Goldan, E. Williams, B. M. Lerner, P. Murphy and F. C. Fehsenfeld, Measurements of PANs during the New England air quality study 2002, *J. Geophys. Res.:Atmos.*, 2007, **112**, D20306.

106 J. Williams, J. M. Roberts, S. B. Bertman, C. A. Stroud, F. C. Fehsenfeld, K. Baumann, M. P. Buhr, K. Knapp, P. C. Murphy, M. Nowick and E. J. Williams, A method for the airborne measurement of PAN, PPN, and MPAN, *J. Geophys. Res.:Atmos.*, 2000, **105**, 28943–28960.

107 G. P. Mills, W. T. Sturges, R. A. Salmon, S. J. B. Bauguitte, K. A. Read and B. J. Bandy, Seasonal variation of peroxyacetylnitrate (PAN) in coastal Antarctica measured with a new instrument for the detection of sub-part per trillion mixing ratios of PAN, *Atmos. Chem. Phys.*, 2007, **7**, 4589–4599.

108 H.-W. Jacobi and O. Schrems, Peroxyacetyl nitrate (PAN) distribution over the South Atlantic Ocean, *Phys. Chem. Chem. Phys.*, 1999, **1**, 5517–5521.

109 J. Williams, J. M. Roberts, S. B. Bertman, C. A. Stroud, F. C. Fehsenfeld, K. Baumann, M. P. Buhr, K. Knapp, P. C. Murphy, M. Nowick and E. J. Williams, A method for the airborne measurement of PAN, PPN, and MPAN, *J. Geophys. Res.:Atmos.*, 2000, **105**, 28943–28960.

110 B. Ridley, J. Walega, G. Hübler, D. Montzka, E. Atlas, D. Hauglustaine, F. Grahek, J. Lind, T. Campos, R. Norton, J. Greenberg, S. Schauffler, S. Oltmans and S. Whittlestone, Measurements of NO and PAN and estimates of O3 production over the seasons during Mauna Loa Observatory Photochemistry Experiment 2, *J. Geophys. Res.:Atmos.*, 1998, **103**, 8323–8339.

111 S. Sandholm, J. Olson, J. Bradshaw, R. Talbot, H. Singh, G. Gregory, D. Blake, B. Anderson, G. Sachse, J. Barrick, J. Collins, K. Klemm, B. Lefer, O. Klemm, K. Gorzelska, D. Herlth and D. O'Hara, Summertime partitioning and budget of NOy compounds in the troposphere over Alaska and Canada: ABLE 3B, *J. Geophys. Res.:Atmos.*, 1994, **99**, 1837–1861.

112 H. B. Singh and L. J. Salas, Methodology for the analysis of Peroxyacetyl nitrate (PAN) in the unpolluted atmosphere, *Atmos. Environ.*, 1983, (17), 1507–1516.

113 J. Rudolph, B. Vierkorn-Rudolph and F. X. Meixner, Large-scale distribution of peroxyacetylnitrate results from the STRATOZ III flights, *J. Geophys. Res.:Atmos.*, 1987, **92**, 6653–6661.

114 G. Lee, H.-S. Choi, T. Lee, J. Choi, J. S. Park and J. Y. Ahn, Variations of regional background peroxyacetyl nitrate in marine boundary layer over Baengyeong Island, South Korea, *Atmos. Environ.*, 2012, **61**, 533–541.

115 J. Gil, M. Lee, J. Han, J.-A. Kim, S. Kim, A. Guenther, H. Kim, S. Kim, S. Lee and D. Kim, Peroxyacetyl Nitrate and Ozone Enhancement at Taehwa Research Forest under the Influence of Seoul Metropolitan Area, *Aerosol Air Qual. Res.*, 2018, **18**, 2262–2273.

116 G. Lee, Y. Jang, H. Lee, J.-S. Han, K.-R. Kim and M. Lee, Characteristic behavior of peroxyacetyl nitrate (PAN) in Seoul megacity, Korea, *Chemosphere*, 2008, **73**, 619–628.

117 M. R. Burkhardt, N. I. Maniga, D. H. Stedman and R. J. Paur, Gas chromatographic method for measuring nitrogen dioxide and peroxyacetyl nitrate in air without compressed gas cylinders, *Anal. Chem.*, 1988, **60**, 816–819.

118 J. D. Lee, A. C. Lewis, P. S. Monks, M. Jacob, J. F. Hamilton, J. R. Hopkins, N. M. Watson, J. E. Saxton, C. Ennis, L. J. Carpenter, N. Carslaw, Z. Fleming, B. J. Bandy, D. E. Oram, S. A. Penkett, J. Slemr, E. Norton, A. R. Rickard, L. K Whalley, D. E. Heard, W. J. Bloss, T. Gravestock, S. C. Smith, J. Stanton, M. J. Pilling and M. E. Jenkin, Ozone photochemistry and elevated isoprene during the UK heatwave of august 2003, *Atmos. Environ.*, 2006, **40**, 7598–7613.

119 E. Atlas and S. Schauffler, Analysis of alkyl nitrates and selected halocarbons in the ambient atmosphere using a charcoal preconcentration technique, *Environ. Sci. Technol.*, 1991, **25**, 61–67.

120 P. Blanchard, P. B. Shepson, K. W. So, H. I. Schiff, J. W. Bottenheim, A. J. Gallant, J. W. Drummond and

 

P. Wong, A comparison of calibration and measurement techniques for gas-chromatographic determination of atmospheric peroxyacetyl nitrate (PAN), *Atmos. Environ., Part A*, 1990, **24**, 2839–2846.

121 F. Flocke, A. Volz-Thomas, H. J. Buers, W. Patz, H. J. Garthe and D. Kley, Long-term measurements of alkyl nitrates in southern Germany 1. General behavior and seasonal and diurnal variation, *J. Geophys. Res.:Atmos.*, 1998, **103**, 5729–5746.

122 M. S. Alam, L. R. Crilley, J. D. Lee, L. J. Kramer, C. Pfrang, M. Vázquez-Moreno, M. Ródenas, A. Muñoz and W. J. Bloss, Interference from alkenes in chemiluminescent NOx measurements, *Atmos. Meas. Tech.*, 2020, **13**, 5977–5991.

123 D. Paul and H. D. Osthoff, Absolute Measurements of Total Peroxy Nitrate Mixing Ratios by Thermal Dissociation Blue Diode Laser Cavity Ring-Down Spectroscopy, *Anal. Chem.*, 2010, **82**, 6695–6703.

124 W. Zheng, F. M. Flocke, G. S. Tyndall, A. Swanson, J. J. Orlando, J. M. Roberts, L. G. Huey and D. J. Tanner, Characterization of a thermal decomposition chemical ionization mass spectrometer for the measurement of peroxy acyl nitrates (PANs) in the atmosphere, *Atmos. Chem. Phys.*, 2011, **11**, 6529–6547.

125 Z. Liu, Y. Wang, D. Gu, C. Zhao, L. G. Huey, R. Stickel, J. Liao, M. Shao, T. Zhu, L. Zeng, S.-C. Liu, C.-C. Chang, A. Amoroso and F. Costabile, Evidence of Reactive Aromatics As a Major Source of Peroxy Acetyl Nitrate over China, *Environ. Sci. Technol.*, 2010, **44**, 7017–7022.

126 D. L. Slusher, L. G. Huey, D. J. Tanner, F. M. Flocke and J. M. Roberts, A thermal dissociation-chemical ionization mass spectrometry (TD-CIMS) technique for the simultaneous measurement of peroxyacyl nitrates and dinitrogen pentoxide, *J. Geophys. Res.:Atmos.*, 2004, **109**, D19315.

127 D. L. Slusher, L. G. Huey, D. J. Tanner, F. M. Flocke and J. M. Roberts, A thermal dissociation–chemical ionization mass spectrometry (TD-CIMS) technique for the simultaneous measurement of peroxyacyl nitrates and dinitrogen pentoxide, *J. Geophys. Res.:Atmos.*, 2004, **109**, D19315.

128 J. N. Crowley, R. Dörich, P. Eger, F. Helleis, I. Tadic, H. Fischer, J. Williams, A. Edtbauer, N. Wang, B. A. Holanda, M. Poehlker, U. Pöschl, A. Pozzer and J. Lelieveld, Peroxy acetyl nitric anhydride (PAN) and peroxy acetic acid (PAA) over the Atlantic west of Africa during CAFE-Africa and the influence of biomass-burning, *Environ. Sci.: Atmos.*, 2025, 620–635.

129 D. A. Day, P. J. Wooldridge, M. B. Dillon, J. A. Thornton and R. C. Cohen, A thermal dissociation laser-induced fluorescence instrument for in situ detection of NO2, peroxy nitrates, alkyl nitrates, and HNO3, *J. Geophys. Res.:Atmos.*, 2002, **107**, 1–14.

130 P. Di Carlo, E. Aruffo, M. Busilacchio, F. Giammaria, C. Dari-Salisburgo, F. Biancofiore, G. Visconti, J. Lee, S. Moller, C. E. Reeves, S. Bauguitte, G. Forster, R. L. Jones and B. Ouyang, Aircraft based four-channel thermal dissociation laser induced fluorescence instrument for simultaneous measurements of $NO_2$, total peroxy nitrate, total alkyl nitrate, and $HNO_3$, *Atmos. Meas. Tech.*, 2013, **6**, 971–980.

131 D. K. Farmer, P. J. Wooldridge and R. C. Cohen, Application of thermal-dissociation laser induced fluorescence (TD-LIF) to measurement of $HNO_3$, Σalkyl nitrates, Σperoxy nitrates, and $NO_2$ fluxes using eddy covariance, *Atmos. Chem. Phys.*, 2006, **6**, 3471–3486.

132 D. W. T. Griffith and G. Schuster, Atmospheric trace gas-analysis using matrix isolation-Fourier transform infrared-spectroscopy, *J. Atmos. Chem.*, 1987, **5**, 59–81.

133 E. C. Tuazon, A. M. Winer and J. N. Pitts, Trace pollutant concentrations in a multiday smog episode in the California South Coast Air Basin by long path length Fourier transform infrared spectroscopy, *Environ. Sci. Technol.*, 1981, **15**, 1232–1237.

134 D. Paul, A. Furgeson and H. D. Osthoff, Measurements of total peroxy and alkyl nitrate abundances in laboratory-generated gas samples by thermal dissociation cavity ring-down spectroscopy, *Rev. Sci. Instrum.*, 2009, **80**, 114101.

135 L. Y. Zhu, V. H. Payne, T. W. Walker, J. R. Worden, Z. Jiang, S. S. Kulawik and E. V. Fischer, PAN in the eastern Pacific free troposphere: A satellite view of the sources, seasonality, interannual variability, and timeline for trend detection, *J. Geophys. Res.:Atmos.*, 2017, **122**, 3614–3629.

136 K. A. Tereszchuk, D. P. Moore, J. J. Harrison, C. D. Boone, M. Park, J. J. Remedios, W. J. Randel and P. F. Bernath, Observations of peroxyacetyl nitrate (PAN) in the upper troposphere by the Atmospheric Chemistry Experiment-Fourier Transform Spectrometer (ACE-FTS), *Atmos. Chem. Phys.*, 2013, **13**, 5601–5613.

137 V. H. Payne, S. S. Kulawik, E. V. Fischer, J. F. Brewer, L. G. Huey, K. Miyazaki, J. R. Worden, K. W. Bowman, E. J. Hintsa, F. Moore, J. W. Elkins and J. J. Calahorrano, Satellite measurements of peroxyacetyl nitrate from the Cross-Track Infrared Sounder: comparison with ATom aircraft measurements, *Atmos. Meas. Tech.*, 2022, **15**, 3497–3511.

138 G. Allen, J. J. Remedios and K. M. Smith, Low temperature mid-infrared cross-sections for peroxyacetyl nitrate (PAN) vapour, *Atmos. Chem. Phys.*, 2005, **5**, 3153–3158.

139 I. E. Gordon, L. S. Rothman, R. J. Hargreaves, R. Hashemi, E. V. Karlovets, F. M. Skinner, E. K. Conway, C. Hill, R. V. Kochanov, Y. Tan, P. Wcislo, A. A. Finenko, K. Nelson, P. F. Bernath, M. Birk, V. Boudon, A. Campargue, K. V. Chance, A. Coustenis, B. J. Drouin, J. M. Flaud, R. R. Gamache, J. T. Hodges, D. Jacquemart, E. J. Mlawer, A. V. Nikitin, V. I. Perevalov, M. Rotger, J. Tennyson, G. C. Toon, H. Tran, V. G. Tyuterev, E. M. Adkins, A. Baker, A. Barbe, E. Canè, A. G. Császár, A. Dudaryonok, O. Egorov, A. J. Fleisher, H. Fleurbaey, A. Foltynowicz, T. Furtenbacher, J. J. Harrison, J. M. Hartmann, V. M. Horneman, X. Huang, T. Karman, J. Karns, S. Kassi, I. Kleiner, V. Kofman, F. Kwabia-Tchana, N. N. Lavrentieva, T. J. Lee, D. A. Long,

A. A. Lukashevskaya, O. M. Lyulin, V. Y. Makhnev, W. Matt, S. T. Massie, M. Melosso, S. N. Mikhailenko, D. Mondelain, H. S. P. Müller, O. V. Naumenko, A. Perrin, O. L. Polyansky, E. Raddaoui, P. L. Raston, Z. D. Reed, M. Rey, C. Richard, R. Tóbiás, I. Sadiek, D. W. Schwenke, E. Starikova, K. Sung, F. Tamassia, S. A. Tashkun, J. Vander Auwera, I. A. Vasilenko, A. A. Vigasin, G. L. Villanueva, B. Vispoel, G. Wagner, A. Yachmenev and S. N. Yurchenko, The HITRAN2020 molecular spectroscopic database, *J. Quant. Spectrosc. Radiat. Transfer*, 2022, **277**, 107949.

140 G. Allen, J. J. Remedios, D. A. Newnham, K. M. Smith and P. S. Monks, Improved mid-infrared cross-sections for peroxyacetyl nitrate (PAN) vapour, *Atmos. Chem. Phys.*, 2005, **5**, 47–56.

141 G. Allen, J. J. Remedios and K. M. Smith, Low temperature mid-infrared cross-sections for peroxyacetyl nitrate (PAN) vapour, *Atmos. Chem. Phys.*, 2005, **5**, 3153–3158.

142 H. Keller-Rudek, G. K. Moortgat, R. Sander and R. Sörensen, The MPI-Mainz UV/VIS Spectral Atlas of Gaseous Molecules of Atmospheric Interest, *Earth Syst. Sci. Data*, 2013, **5**, 365–373.

143 G. I. Senum, Y. N. Lee and J. S. Gaffney, Ultraviolet absorption spectrum of peroxyacetyl nitrate and peroxypropionyl nitrate, *J. Phys. Chem.*, 1984, **88**, 1269–1270.

144 H. G. Libuda and F. Zabel, UV absorption cross-sections of acetyl peroxynitrate and trifluoroacetyl peroxynitrate at 298 K, *Ber. Bunsen-Ges.*, 1995, **99**, 1205–1213.

145 N. Basco and S. S. Parmar, The reaction of acetylperoxy radicals with NO2, *Int. J. Chem. Kinet.*, 1987, **19**, 115–128.

146 R. Atkinson, D. L. Baulch, R. A. Cox, J. N. Crowley, R. F. Hampson, R. G. Hynes, M. E. Jenkin, M. J. Rossi, J. Troe and I. Subcommittee, Evaluated kinetic and photochemical data for atmospheric chemistry: Volume II – gas phase reactions of organic species, *Atmos. Chem. Phys.*, 2006, **6**, 3625–4055.

147 J. B. Burkholder, S. P. Sander, J. P. D. Abbatt, J. R. Barker, C. Cappa, J. D. Crounse, T. S. Dibble, R. E. Huie, C. E. Kolb, M. J. Kurylo, V. L. Orkin, C. J. Percival, D. M. Wilmouth, P. H. Wine, *Chemical Kinetics and Photochemical Data for Use in Atmospheric Studies, Evaluation No. 17, JPL Publication 19-5*, Jet Propulsion Laboratory, Pasadena, 2011.

148 E. R. Stephens, The formation, reactions, and properties of peroxyacyl nitrates (PANs) in photochemical air pollution, *Adv. Environ. Sci. Technol.*, 1969, **1**, 119–146.

149 R. R. E. P. Roth, G. Moorgat, R. Meller and W. Schneider, *Absoprtion spectrum of PAN ($CH_3C(O)O_2NO_2$)*, 1981.

150 D. Grosjean and E. L. Williams Ii, Photochemical Pollution at Two Southern California Smog Receptor Sites, *J. Air Waste Manage. Assoc.*, 1992, **42**, 805–809.

151 A. Hansel and A. Wisthaler, A method for real-time detection of PAN, PPN and MPAN in ambient air, *Geophys. Res. Lett.*, 2000, **27**, 895–898.

152 A. M. Dunker, S. Kumar and P. H. Berzins, A comparison of chemical mechanisms used in atmospheric models, *Atmos. Environ.*, 1984, (18), 311–321.

153 R. A. Kotchenruther, D. A. Jaffe and L. Jaeglé, Ozone photochemistry and the role of peroxyacetyl nitrate in the springtime northeastern Pacific troposphere: Results from the Photochemical Ozone Budget of the Eastern North Pacific Atmosphere (PHOBEA) campaign, *J. Geophys. Res.:Atmos.*, 2001, **106**, 28731–28742.

154 C. C. van Heerwaarden, J. Vilà-Guerau de Arellano and A. J. Teuling, Land-atmosphere coupling explains the link between pan evaporation and actual evapotranspiration trends in a changing climate, *Geophys. Res. Lett.*, 2010, **37**, L21401.

155 W. P. L. Carter, A. M. Winer and J. N. Pitts, Effect of peroxyacetyl nitrate on the initiation of photochemical smog, *Environ. Sci. Technol.*, 1981, **15**, 831–834.

156 N. A. Kelly, A captive-air irradiation study of the response of nitric acid and peroxyacetyl nitrate to ozone control strategies in Los Angeles, *Atmos. Environ., Part B*, 1992, **26**, 463–472.

157 T. Liu, Y. Wang, H. Cai, H. Wang, C. Zhang, J. Chen, Y. Dai, W. Zhao, J. Li, D. Gong, D. Chen, Y. Zhai, Y. Zhou, T. Liao and B. Wang, Complexities of peroxyacetyl nitrate photochemistry and its control strategies in contrasting environments in the Pearl River Delta region, *npj Clim. Atmos. Sci.*, 2024, **7**, 116.

158 B. Hu, N. Chen, R. Li, M. Huang, J. Chen, Y. Hong, L. Xu, X. Fan, M. Li, L. Tong, Q. Zheng and Y. Yang, Understanding summertime peroxyacetyl nitrate (PAN) formation and its relation to aerosol pollution: insights from high-resolution measurements and modeling, *Atmos. Chem. Phys.*, 2025, **25**, 905–921.

159 S. Fadnavis, K. Semeniuk, M. G. Schultz, M. Kiefer, A. Mahajan, L. Pozzoli and S. Sonbawane, Transport pathways of peroxyacetyl nitrate in the upper troposphere and lower stratosphere from different monsoon systems during the summer monsoon season, *Atmos. Chem. Phys.*, 2015, **15**, 11477–11499.

160 J. S. Gaffney, N. A. Marley, R. S. Martin, R. W. Dixon, L. G. Reyes and C. J. Popp, Potential Air Quality Effects of Using Ethanol−Gasoline Fuel Blends: A Field Study in Albuquerque, New Mexico, *Environ. Sci. Technol.*, 1997, **31**, 3053–3061.

161 D. Grosjean, Atmospheric Chemistry of Toxic Contaminants. 2. Saturated Aliphatics: Acetaldehyde, Dioxane, Ethylene Glycol Ethers, Propylene Oxide, *J. Air Waste Manage. Assoc.*, 1990, **40**, 1522–1531.

162 M. Sun, J. n. Cui, X. Zhao and J. Zhang, Impacts of precursors on peroxyacetyl nitrate (PAN) and relative formation of PAN to ozone in a southwestern megacity of China, *Atmos. Environ.*, 2020, **231**, 117542.

163 J. M. Roberts, J. Williams, K. Baumann, M. P. Buhr, P. D. Goldan, J. Holloway, G. Hübler, W. C. Kuster, S. A. McKeen, T. B. Ryerson, M. Trainer, E. J. Williams, F. C. Fehsenfeld, S. B. Bertman, G. Nouaime, C. Seaver, G. Grodzinsky, M. Rodgers and V. L. Young, Measurements of PAN, PPN, and MPAN made during the 1994 and 1995 Nashville Intensives of the Southern Oxidant Study: Implications for regional ozone

 

production from biogenic hydrocarbons, *J. Geophys. Res.:Atmos.*, 1998, **103**, 22473–22490.

164 J. Williams, J. M. Roberts, F. C. Fehsenfeld, S. B. Bertman, M. P. Buhr, P. D. Goldan, G. Hübler, W. C. Kuster, T. B. Ryerson, M. Trainer and V. Young, Regional ozone from biogenic hydrocarbons deduced from airborne measurements of PAN, PPN, and MPAN, *Geophys. Res. Lett.*, 1997, **24**, 1099–1102.

165 H. B. Singh and L. J. Salas, Measurements of peroxyacetyl nitrate (pan) and peroxypropionyl nitrate (ppn) at selected urban, rural and remote sites, *Atmos. Environ.*, 1989, (23), 231–238.

166 M. Claeys and W. Maenhaut, Secondary Organic Aerosol Formation from Isoprene: Selected Research, Historic Account and State of the Art, *Atmosphere*, 2021, **12**, 728.

167 Y.-H. Lin, H. Zhang, H. O. T. Pye, Z. Zhang, W. J. Marth, S. Park, M. Arashiro, T. Cui, S. H. Budisulistiorini, K. G. Sexton, W. Vizuete, Y. Xie, D. J. Luecken, I. R. Piletic, E. O. Edney, L. J. Bartolotti, A. Gold and J. D. Surratt, Epoxide as a precursor to secondary organic aerosol formation from isoprene photooxidation in the presence of nitrogen oxides, *Proc. Natl. Acad. Sci. U. S. A.*, 2013, **110**, 6718–6723.

168 M. Sun, Y. Zhou, Y. Wang, X. Qiao, J. Wang and J. Zhang, Heterogeneous Reaction of Peroxyacetyl Nitrate on Real-World PM2.5 Aerosols: Kinetics, Influencing Factors, and Atmospheric Implications, *Environ. Sci. Technol.*, 2022, **56**, 9325–9334.

169 W. Xu, G. Zhang, Y. Wang, S. Tong, W. Zhang, Z. Ma, W. Lin, Y. Kuang, L. Yin and X. Xu, Aerosol Promotes Peroxyacetyl Nitrate Formation During Winter in the North China Plain, *Environ. Sci. Technol.*, 2021, **55**, 3568–3581.

170 H. Zhu, T. Gao and J. Zhang, Wintertime characteristic of peroxyacetyl nitrate in the Chengyu district of southwestern China, *Environ. Sci. Pollut. Res.*, 2018, **25**, 23143–23156.

171 M. Olin, M. Okuljar, M. P. Rissanen, J. Kalliokoski, J. Shen, L. Dada, M. Lampimäki, Y. Wu, A. Lohila, J. Duplissy, M. Sipilä, T. Petäjä, M. Kulmala and M. Dal Maso, Measurement report: Atmospheric new particle formation in a coastal agricultural site explained with binPMF analysis of nitrate CI-APi-TOF spectra, *Atmos. Chem. Phys.*, 2022, **22**, 8097–8115.

172 N. Fu, L.-M. Cao, S.-Y. Xia, L.-W. Zeng, L. He, L.-Y. He and X.-F. Huang, Sensitivity of atmospheric peroxyacetyl nitrate (PAN) formation and its impact on ozone pollution in a coastal city, *Atmos. Environ.*, 2024, **330**, 120545.

173 E. Grosjean, D. Grosjean, M. P. Fraser and G. R. Cass, Air Quality Model Evaluation Data for Organics. 3. Peroxyacetyl Nitrate and Peroxypropionyl Nitrate in Los Angeles Air, *Environ. Sci. Technol.*, 1996, **30**, 2704–2714.

174 E. L. Williams, E. Grosjean and D. Grosjean, Ambient levels of the peroxyacyl nitrates PAN, PPN and MPAN in Atlanta, Georgia, *J. Air Waste Manage. Assoc.*, 1993, **43**, 873–879.

175 E. Peake and H. S. Sandhu, The formation of ozone and peroxyacetyl nitrate (PAN) in the urban atmospheres of Alberta, *Can. J. Chem.*, 1983, **61**, 927–935.

176 E. Peake, M. A. MacLean, P. F. Lester and H. S. Sandhu, Peroxyacetylnitrate (PAN) in the atmosphere of Edmonton, Alberta, Canada, *Atmos. Environ.*, 1988, (22), 973–981.

177 E. Tsani-Bazaca, S. Glavas and H. Güsten, Peroxyacetyl nitrate (PAN) concentrations in Athens, Greece, *Atmos. Environ.*, 1988, (22), 2283–2286.

178 B. A. Ridley, J. D. Shetter, J. G. Walega, S. Madronich, C. M. Elsworth, F. E. Grahek, F. C. Fehsenfeld, R. B. Norton, D. D. Parrish, G. Hübler, M. Buhr, E. J. Williams, E. J. Allwine and H. H. Westberg, The behavior of some organic nitrates at Boulder and Niwot Ridge, Colorado, *J. Geophys. Res.:Atmos.*, 1990, **95**, 13949–13961.

179 N. Tsalkani, P. Perros, A. L. Dutot and G. Toupance, One-year measurements of PAN in the Paris basin: Effect of meteorological parameters, *Atmos. Environ., Part A*, 1991, **25**, 1941–1949.

180 S. Wunderli and R. Gehrig, Influence of temperature on formation and stability of surface pan and ozone - a 2-year field-study in Switzerland, *Atmos. Environ., Part A*, 1991, **25**, 1599–1608.

181 J. G. Walega, B. A. Ridley, S. Madronich, F. E. Grahek, J. D. Shetter, T. D. Sauvain, C. J. Hahn, J. T. Merill, B. A. Bodhaine and E. Robinson, Observations of peroxyacetyl nitrate, peroxypropionyl nitrate, methyl nitrate and ozone during the Mauna Loa Observatory photochemistry experiment, *J. Geophys. Res.:Atmos.*, 1992, **97**, 10311–10330.

182 R. Schmitt and A. Volz-Thomas, Climatology of Ozone, PAN, CO, and NMHC in the Free Troposphere Over the Southern North Atlantic, *J. Atmos. Chem.*, 1997, **28**, 245–262.

183 B. A. Ridley, E. L. Atlas, J. G. Walega, G. L. Kok, T. A. Staffelbach, J. P. Greenberg, F. E. Grahek, P. G. Hess and D. D. Montzka, Aircraft measurements made during the spring maximum of ozone over Hawaii: Peroxides, CO, O-3, NOy, condensation nuclei, selected hydrocarbons, halocarbons, and alkyl nitrates between 0.5 and 9 km altitude, *J. Geophys. Res.:Atmos.*, 1997, **102**, 18935–18961.

184 M. P. Buhr, K. J. Hsu, C. M. Liu, R. Liu, L. Wei, Y. C. Liu and Y. S. Kuo, Trace gas measurements and air mass classification from a ground station in Taiwan during the PEM-West A experiment (1991), *J. Geophys. Res.:Atmos.*, 1996, **101**, 2025–2035.

185 I. Ziomas, P. Suppan, B. Rappenglück, D. S. Balis, P. Tzoumaka, D. Melas, A. Papayannis, P. Fabian and C. S. Zerefos, A contribution to the study of photochemical smog in the Greater Athens Area, *Contrib. Atmos. Phys.*, 1995, **68**, 191–203.

186 G. Nouaime, S. B. Bertman, C. Seaver, D. Elyea, H. Huang, P. B. Shepson, T. K. Starn, D. D. Riemer, R. G. Zika and K. Olszyna, Sequential oxidation products from tropospheric isoprene chemistry: MACR and MPAN at a NO -rich forest environment in the southeastern United States, *J. Geophys. Res.:Atmos.*, 1998, **103**, 22463–22471.

187 B. Rappenglück, P. Oyola, I. Olaeta and P. Fabian, The Evolution of Photochemical Smog in the Metropolitan Area of Santiago de Chile, *J. Appl. Meteorol.*, 2000, **39**, 275–290.

188 J. S. Gaffney, N. A. Marley, M. M. Cunningham and P. V. Doskey, Measurements of peroxyacyl nitrates (PANS) in Mexico City: implications for megacity air quality impacts on regional scales, *Atmos. Environ.*, 1999, **33**, 5003–5012.

189 N. A. Marley, J. S. Gaffney, R. Ramos-Villegas and B. Cárdenas González, Comparison of measurements of peroxyacyl nitrates and primary carbonaceous aerosol concentrations in Mexico City determined in 1997 and 2003, *Atmos. Chem. Phys.*, 2007, **7**, 2277–2285.

190 E. Grosjean, D. Grosjean and L. F. Woodhouse, Peroxyacetyl Nitrate and Peroxypropionyl Nitrate during SCOS 97-NARSTO, *Environ. Sci. Technol.*, 2001, **35**, 4007–4014.

191 C. Zellweger, M. Ammann, B. Buchmann, P. Hofer, M. Lugauer, R. Rüttimann, N. Streit, E. Weingartner and U. Baltensperger, Summertime $NO_y$ speciation at the Jungfraujoch, 3580 m above sea level, Switzerland, *J. Geophys. Res.:Atmos.*, 2000, **105**, 6655–6667.

192 J. M. Roberts, F. Flocke, A. Weinheimer, H. Tanimoto, B. J. Jobson, D. Riemer, E. Apel, E. Atlas, S. Donnelly, V. Stroud, K. Johnson, R. Weaver and F. C. Fehsenfeld, Observations of APAN during TexAQS 2000, *Geophys. Res. Lett.*, 2001, **28**, 4195–4198.

193 J. M. Roberts, B. T. Jobson, W. Kuster, P. Goldan, P. Murphy, E. Williams, G. Frost, D. Riemer, E. Apel, C. Stroud, C. Wiedinmyer and F. Fehsenfeld, An examination of the chemistry of peroxycarboxylic nitric anhydrides and related volatile organic compounds during Texas Air Quality Study 2000 using ground-based measurements, *J. Geophys. Res.:Atmos.*, 2003, **108**, 4495.

194 J. M. Roberts, F. Flocke, C. A. Stroud, D. Hereid, E. Williams, F. Fehsenfeld, W. Brune, M. Martinez and H. Harder, Ground-based measurements of peroxycarboxylic nitric anhydrides (PANs) during the 1999 Southern Oxidants Study Nashville Intensive, *J. Geophys. Res.:Atmos.*, 2002, **107**, 4554.

195 L. K. Whalley, A. C. Lewis, J. B. McQuaid, R. M. Purvis, J. D. Lee, K. Stemmler, C. Zellweger and P. Ridgeon, Two high-speed, portable GC systems designed for the measurement of non-methane hydrocarbons and PAN: Results from the Jungfraujoch High Altitude Observatory, *J. Environ. Monit.*, 2004, **6**, 234–241.

196 J. M. B. Lööv, S. Henne, G. Legreid, J. Staehelin, S. Reimann, A. S. H. Prévôt, M. Steinbacher and M. K. Vollmer, Estimation of background concentrations of trace gases at the Swiss Alpine site Jungfraujoch (3580 m asl), *J. Geophys. Res.:Atmos.*, 2008, **113**, D22305.

197 J. M. Zhang, T. Wang, A. J. Ding, X. H. Zhou, L. K. Xue, C. N. Poon, W. S. Wu, J. Gao, H. C. Zuo, J. M. Chen, X. C. Zhang and S. J. Fan, Continuous measurement of peroxyacetyl nitrate (PAN) in suburban and remote areas of western China, *Atmos. Environ.*, 2009, **43**, 228–237.

198 B. W. LaFranchi, G. M. Wolfe, J. A. Thornton, S. A. Harrold, E. C. Browne, K. E. Min, P. J. Wooldridge, J. B. Gilman, W. C. Kuster, P. D. Goldan, J. A. de Gouw, M. McKay, A. H. Goldstein, X. Ren, J. Mao and R. C. Cohen, Closing the peroxy acetyl nitrate budget: observations of acyl peroxy nitrates (PAN, PPN, and MPAN) during BEARPEX 2007, *Atmos. Chem. Phys.*, 2009, **9**, 7623–7641.

199 S. Pandey Deolal, S. Henne, L. Ries, S. Gilge, U. Weers, M. Steinbacher, J. Staehelin and T. Peter, Analysis of elevated springtime levels of Peroxyacetyl nitrate (PAN) at the high Alpine research sites Jungfraujoch and Zugspitze, *Atmos. Chem. Phys.*, 2014, **14**, 12553–12571.

200 S. Pandey Deolal, J. Staehelin, D. Brunner, J. Cui, M. Steinbacher, C. Zellweger, S. Henne and M. K. Vollmer, Transport of PAN and NOy from different source regions to the Swiss high alpine site Jungfraujoch, *Atmos. Environ.*, 2013, **64**, 103–115.

201 X. Xu, H. Zhang, W. Lin, Y. Wang, W. Xu and S. Jia, First simultaneous measurements of peroxyacetyl nitrate (PAN) and ozone at Nam Co in the central Tibetan Plateau: impacts from the PBL evolution and transport processes, *Atmos. Chem. Phys.*, 2018, **18**, 5199–5217.

202 H. L. Zhu, T. Y. Gao and J. B. Zhang, Wintertime characteristic of peroxyacetyl nitrate in the Chengyu district of southwestern China, *Environ. Sci. Pollut. Res.*, 2018, **25**, 23143–23156.

203 J. Zaragoza, S. Callahan, E. E. McDuffie, J. Kirkland, P. Brophy, L. Durrett, D. K. Farmer, Y. Zhou, B. Sive, F. Flocke, G. Pfister, C. Knote, A. Tevlin, J. Murphy and E. V. Fischer, Observations of Acyl Peroxy Nitrates During the Front Range Air Pollution and Photochemistry Experiment (FRAPPE), *J. Geophys. Res.:Atmos.*, 2017, **122**, 12416–12432.

204 Y. Qiu, W. Lin, K. Li, L. Chen, Q. Yao, Y. Tang and Z. Ma, Vertical characteristics of peroxyacetyl nitrate (PAN) from a 250-m tower in northern China during September 2018, *Atmos. Environ.*, 2019, **213**, 55–63.

205 Z. Y. Li, G. Z. Xie, H. Chen, B. X. Zhan, L. Wang, Y. J. Mu, A. Mellouki and J. M. Chen, Characterization of peroxyacetyl nitrate (PAN) under different PM2.5 concentration in wintertime at a North China rural site, *J. Environ. Sci.*, 2022, **114**, 221–232.

206 Y. Liu, H. Shen, J. Mu, H. Li, T. Chen, J. Yang, Y. Jiang, Y. Zhu, H. Meng, C. Dong, W. Wang and L. Xue, Formation of peroxyacetyl nitrate (PAN) and its impact on ozone production in the coastal atmosphere of Qingdao, North China, *Sci. Total Environ.*, 2021, **778**, 146265.

207 D. Grosjean, E. L. Williams and E. Grosjean, Peroxyacyl nitrates at southern California mountain forest locations, *Environ. Sci. Technol.*, 1993, **27**, 110–121.

208 H. B. Singh and P. L. Hanst, Peroxyacetyl nitrate (PAN) in the unpolluted atmosphere: An important reservoir for nitrogen oxides, *Geophys. Res. Lett.*, 1981, **8**, 941–944.

209 E. V. Fischer, D. A. Jaffe and E. C. Weatherhead, Free tropospheric peroxyacetyl nitrate (PAN) and ozone at Mount Bachelor: potential causes of variability and

timescale for trend detection, *Atmos. Chem. Phys.*, 2011, **11**, 5641–5654.

210 R. Corkum, W. W. Giesbrecht, T. Bardsley and E. A. Cherniak, Peroxyacetyl nitrate (PAN) in the atmosphere at Simcoe, Canada, *Atmos. Environ.*, 1986, (20), 1241–1248.

211 I. Watanabe, M. Nakanishi, J. Tomita, S. Hatakeyama, K. Murano, H. Mukai and H. Bandou, Atmospheric peroxyacyl nitrates in urban/remote sites and the lower troposphere around Japan, *Environ. Pollut.*, 1998, **102**, 253–261.

212 H. B. Singh, E. Condon, J. Vedder, D. O'Hara, B. A. Ridley, B. W. Gandrud, J. D. Shetter, L. J. Salas, B. Huebert, G. Hübler, M. A. Carroll, D. L. Albritton, D. D. Davis, J. D. Bradshaw, S. T. Sandholm, M. O. Rodgers, S. M. Beck, G. L. Gregory and P. J. LeBel, Peroxyacetyl nitrate measurements during CITE 2: Atmospheric distribution and precursor relationships, *J. Geophys. Res.:Atmos.*, 1990, **95**, 10163–10178.

213 H. B. Singh, D. Herlth, D. O'Hara, L. Salas, A. L. Torres, G. L. Gregory, G. W. Sachse and J. F. Kasting, Atmospheric peroxyacetyl nitrate measurements over the Brazilian Amazon Basin during the wet season: Relationships with nitrogen oxides and ozone, *J. Geophys. Res.:Atmos.*, 1990, **95**, 16945–16954.

214 J. S. Gaffney, N. A. Marley and E. W. Prestbo, Measurements of peroxyacetyl nitrate at a remote site in the southwestern United States: tropospheric implications, *Environ. Sci. Technol.*, 1993, **27**, 1905–1910.

215 E. L. Williams and D. Grosjean, Peroxypropionyl nitrate at a southern California mountain forest site, *Environ. Sci. Technol.*, 1991, **25**, 653–659.

216 D. J. J. S.-M. Fan, D. L. Mauzerall, J. D. Bradshaw, S. T. Sandholm, D. R. Blake, H. B. Singh, R. W. Talbot, G. L. Gregory and G. W. Sachse, Origin of tropospheric NO over subarctic eastern Canada in summer, *J. Geophys. Res.:Atmos.*, 1994, **99**, 16867–16877.

217 R. W. Talbot, J. D. Bradshaw, S. T. Sandholm, H. B. Singh, G. W. Sachse, J. Collins, G. L. Gregory, B. Anderson, D. Blake, J. Barrick, E. V. Browell, K. I. Klemm, B. L. Lefer, O. Klemm, K. Gorzelska, J. Olson, D. Herlth and D. O'Hara, Summertime distribution and relations of reactive odd nitrogen species and NOy in the troposphere over Canada, *J. Geophys. Res.:Atmos.*, 1994, **99**, 1863–1885.

218 H. B. Singh, D. Herlth, D. O'Hara, K. Zahnle, J. D. Bradshaw, S. T. Sandholm, R. Talbot, G. L. Gregory, G. W. Sachse, D. R. Blake and S. C. Wofsy, Summertime distribution of PAN and other reactive nitrogen species in the northern high-latitude atmosphere of eastern Canada, *J. Geophys. Res.:Atmos.*, 1994, **99**, 1821–1835.

219 P. Perros, Large-scale distribution of peroxyacetylnitrate from aircraft measurements during the TROPOZ II experiment, *J. Geophys. Res.:Atmos.*, 1994, **99**, 8269–8279.

220 D. R. Hastie, P. B. Shepson, N. Reid, P. B. Roussel and O. T. Melo, Summertime NOx, NOy, and ozone at a site in rural Ontario, *Atmos. Environ.*, 1996, **30**, 2157–2165.

221 H. B. Singh, D. Herlth, R. Kolyer, R. Chatfield, W. Viezee, L. J. Salas, Y. Chen, J. D. Bradshaw, S. T. Sandholm, R. Talbot, G. L. Gregory, B. Anderson, G. W. Sachse, E. Browell, A. S. Bachmeier, D. R. Blake, B. Heikes, D. Jacob and H. E. Fuelberg, Impact of biomass burning emissions on the composition of the South Atlantic troposphere: Reactive nitrogen and ozone, *J. Geophys. Res.:Atmos.*, 1996, **101**, 24203–24219.

222 I. Fenneteaux, P. Colin, A. Etienne, H. Boudries, A. L. Dutot, P. E. Perros and G. Toupance, Influence of Continental Sources on Oceanic Air Composition at the Eastern Edge of the North Atlantic Ocean, TOR 1992–1995, *J. Atmos. Chem.*, 1999, **32**, 233–280.

223 G. G. McFadyen and J. N. Cape, Peroxyacetyl nitrate in eastern Scotland, *Sci. Total Environ.*, 2005, **337**, 213–222.

224 E. Grosjean, D. Grosjean, L. F. Woodhouse and Y.-J. Yang, Peroxyacetyl nitrate and peroxypropionyl nitrate in Porto Alegre, Brazil, *Atmos. Environ.*, 2002, **36**, 2405–2419.

225 D. Jaffe, T. Anderson, D. Covert, B. Trost, J. Danielson, W. Simpson, D. Blake, J. Harris and D. Streets, Observations of ozone and related species in the northeast Pacific during the PHOBEA campaigns: 1. Ground-based observations at Cheeka Peak, *J. Geophys. Res.:Atmos.*, 2001, **106**, 7449–7461.

226 T. Thornberry, M. A. Carroll, G. J. Keeler, S. Sillman, S. B. Bertman, M. R. Pippin, K. Ostling, J. W. Grossenbacher, P. B. Shepson, O. R. Cooper, J. L. Moody and W. R. Stockwell, Observations of reactive oxidized nitrogen and speciation of NO during the PROPHET summer 1998 intensive, *J. Geophys. Res.:Atmos.*, 2001, **106**, 24359–24386.

227 H. Tanimoto, H. Furutani, S. Kato, J. Matsumoto, Y. Makide and H. Akimoto, Seasonal cycles of ozone and oxidized nitrogen species in northeast Asia - 1. Impact of regional climatology and photochemistry observed during RISOTTO 1999-2000, *J. Geophys. Res.:Atmos.*, 2002, **107**, 4747.

228 Y. Huang, S. Wu, L. J. Kramer, D. Helmig and R. E. Honrath, Surface ozone and its precursors at Summit, Greenland: comparison between observations and model simulations, *Atmos. Chem. Phys.*, 2017, **17**, 14661–14674.

229 Z. Xu, L. Xue, T. Wang, T. Xia, Y. Gao, P. K. K. Louie and C. W. Y. Luk, Measurements of Peroxyacetyl Nitrate at a Background Site in the Pearl River Delta Region: Production Efficiency and Regional Transport, *Aerosol Air Qual. Res.*, 2015, **15**, 833–841.

230 J. M. Roberts, F. Flocke, G. Chen, J. de Gouw, J. S. Holloway, G. Hübler, J. A. Neuman, D. K. Nicks, J. B. Nowak, D. D. Parrish, T. B. Ryerson, D. T. Sueper, C. Warneke and F. C. Fehsenfeld, Measurement of peroxycarboxylic nitric anhydrides (PANs) during the ITCT 2K2 aircraft intensive experiment -: art. no. D23S21, *J. Geophys. Res.:Atmos.*, 2004, **109**, D23S21.

231 J. W. Bottenheim, A. Sirois, K. A. Brice and A. J. Gallant, Five years of continuous observations of PAN and ozone at a rural location in eastern Canada, *J. Geophys. Res.:Atmos.*, 1994, **99**, 5333–5352.

232 L. A. Barrie, G. den Hartog, J. W. Bottenheim and S. Landsberger, Anthropogenic aerosols and gases in the lower troposphere at Alert Canada in April 1986, *J. Atmos. Chem.*, 1989, **9**, 101–127.

233 J. W. Bottenheim, L. A. Barrie and E. Atlas, The partitioning of nitrogen oxides in the lower Arctic troposphere during spring 1988, *J. Atmos. Chem.*, 1993, **17**, 15–27.

234 H. J. Beine, D. A. Jaffe, D. R. Blake, E. Atlas and J. Harris, Measurements of PAN, alkyl nitrates, ozone, and hydrocarbons during spring in interior Alaska, *J. Geophys. Res.:Atmos.*, 1996, **101**, 12613–12619.

235 S. Solberg, T. Krognes, F. Stordal, O. Hov, H. J. Beine, D. A. Jaffe, K. C. Clemitshaw and S. A. Penkett, Reactive Nitrogen Compounds at Spitsbergen in the Norwegian Arctic, *J. Atmos. Chem.*, 1997, **28**, 209–225.

236 H. J. Beine and T. Krognes, The seasonal cycle of peroxyacetyl nitrate (PAN) in the European Arctic, *Atmos. Environ.*, 2000, **34**, 933–940.

237 H. J. Beine, D. A. Jaffe, J. A. Herring, J. A. Kelley, T. Krognes and F. Stordal, High-latitude springtime photochemistry. 1. NOx, PAN and ozone relationships, *J. Atmos. Chem.*, 1997, **27**, 127–153.

238 K. M. Ford, B. M. Campbell, P. B. Shepson, S. B. Bertman, R. E. Honrath, M. Peterson and J. E. Dibb, Studies of Peroxyacetyl nitrate (PAN) and its interaction with the snowpack at Summit, Greenland, *J. Geophys. Res.:Atmos.*, 2002, **107**, D104102.

239 H. W. Jacobi, R. Weller, A. E. Jones, P. S. Anderson and O. Schrems, Peroxyacetyl nitrate (PAN) concentrations in the Antarctic troposphere measured during the photochemical experiment at Neumayer (PEAN'99), *Atmos. Environ.*, 2000, **34**, 5235–5247.

240 H. B. Singh, D. Herlth, R. Kolyer, L. Salas, J. D. Bradshaw, S. T. Sandholm, D. D. Davis, J. Crawford, Y. Kondo, M. Koike, R. Talbot, G. L. Gregory, G. W. Sachse, E. Browell, D. R. Blake, F. S. Rowland, R. Newell, J. Merrill, B. Heikes, S. C. Liu, P. J. Crutzen and M. Kanakidou, Reactive nitrogen and ozone over the western Pacific: Distribution, partitioning, and sources, *J. Geophys. Res.:Atmos.*, 1996, **101**, 1793–1808.

241 H. B. Singh, W. Viezee, Y. Chen, A. N. Thakur, Y. Kondo, R. W. Talbot, G. L. Gregory, G. W. Sachse, D. R. Blake, J. D. Bradshaw, Y. Wang and D. J. Jacob, Latitudinal distribution of reactive nitrogen in the free troposphere over the Pacific Ocean in late winter/early spring, *J. Geophys. Res.:Atmos.*, 1998, **103**, 28237–28246.

242 H. W. Jacobi, R. Weller, T. Bluszcz and O. Schrems, Latitudinal distribution of peroxyacetyl nitrate (PAN) over the Atlantic Ocean, *J. Geophys. Res.:Atmos.*, 1999, **104**, 26901–26912.

243 R. A. Kotchenruther, D. A. Jaffe, H. J. Beine, T. L. Anderson, J. W. Bottenheim, J. M. Harris, D. R. Blake and R. Schmitt, Observations of ozone and related species in the northeast Pacific during the PHOBEA campaigns: 2. Airborne observations, *J. Geophys. Res.:Atmos.*, 2001, **106**, 7463–7483.

244 R. S. Russo, R. W. Talbot, J. E. Dibb, E. Scheuer, G. Seid, C. E. Jordan, H. E. Fuelberg, G. W. Sachse, M. A. Avery, S. A. Vay, D. R. Blake, N. J. Blake, E. Atlas, A. Fried, S. T. Sandholm, D. Tan, H. B. Singh, J. Snow and B. G. Heikes, Chemical composition of Asian continental outflow over the western Pacific: Results from Transport and Chemical Evolution over the Pacific (TRACE-P), *J. Geophys. Res.:Atmos.*, 2003, **108**, 8804.

245 A. Fischer, S. Langer and E. Ljungström, Chemistry and indoor air quality in a multi-storey wooden passive (low energy) building: Formation of peroxyacetyl nitrate, *Indoor Built Environ.*, 2013, **23**, 485–496.

246 M. W. M. Hisham and D. Grosjean, Sulfur dioxide, hydrogen sulfide, total reduced sulfur, chlorinated hydrocarbons and photochemical oxidants in southern California museums, *Atmos. Environ., Part A*, 1991, **25**, 1497–1505.

247 G. Jakobi and P. Fabian, Indoor/outdoor concentrations of ozone and peroxyacetyl nitrate (PAN), *Int. J. Biometeorol.*, 1997, **40**, 162–165.

248 M. W. M. Hisham and D. Grosjean, Air pollution in southern California museums: indoor and outdoor levels of nitrogen dioxide, peroxyacetyl nitrate, nitric acid, and chlorinated hydrocarbons, *Environ. Sci. Technol.*, 1991, **25**, 857–862.

249 A. P. Altshuller, PANs in the Atmosphere, *Air Waste*, 1993, **43**, 1221–1230.

250 B. Y. Hu, N. H. Chen, R. Li, M. Q. Huang, J. S. Chen, Y. W. Hong, L. L. Xu, X. L. Fan, M. R. Li, L. Tong, Q. P. Zheng and Y. X. Yang, Understanding summertime peroxyacetyl nitrate (PAN) formation and its relation to aerosol pollution: insights from high-resolution measurements and modeling, *Atmos. Chem. Phys.*, 2025, **25**, 905–921.

251 D. Grosjean, E. Grosjean and E. L. Williams, Fading of artists' colorants by a mixture of photochemical oxidants, *Atmos. Environ., Part A*, 1993, **27**, 765–772.

252 H. I. Schiff, G. I. Mackay, C. Castledine, G. W. Harris and Q. Tran, Atmospheric measurements of nitrogen dioxide with a sensitive luminol instrument, *Water, Air, Soil Pollut.*, 1986, **30**, 105–114.

253 M. Kruza, D. Shaw, J. Shaw and N. Carslaw, Towards improved models for indoor air chemistry: A Monte Carlo simulation study, *Atmos. Environ.*, 2021, **262**, 118625.

254 E. Harding-Smith, H. L. Davies, C. O'Leary, R. Winkless, M. Shaw, T. Dillon, B. Jones and N. Carslaw, The impact of surfaces on indoor air chemistry following cooking and cleaning, *Environ. Sci.: Processes Impacts*, 2025, 1583–1602.

255 H. L. Davies, C. O'Leary, T. Dillon, D. R. Shaw, M. Shaw, A. Mehra, G. Phillips and N. Carslaw, A measurement and modelling investigation of the indoor air chemistry following cooking activities, *Environ. Sci.: Processes Impacts*, 2023, **25**, 1532–1548.

 